AMERICAN MUSEUM NOVITATES

Number 3963, 37 pp. January 13, 2021

A new dichromatic species of *Myotis* (Chiroptera: Vespertilionidae) from the Nimba Mountains, Guinea

NANCY B. SIMMONS,[1] JON FLANDERS,[1, 2] ERIC MOÏSE BAKWO FILS,[3] GUY PARKER,[4] JAMISON D. SUTER,[4] SEINAN BAMBA,[4] MORY DOUNO,[5] MAMADY KOBELE KEITA,[6] ARIADNA E. MORALES,[1,7] AND WINIFRED F. FRICK[2, 8]

ABSTRACT

The genus *Myotis* is a diverse group of vespertilionid bats found on nearly every continent. One clade in this group, the subgenus *Chrysopteron*, is characterized by reddish to yellowish fur and, in some cases, visually striking dichromatic wing pigmentation. Here, we describe a new dichromatic species of *Myotis* (*Chrysopteron*) from the Nimba Mountains in Guinea. The new species is superficially similar to *Myotis welwitschii*, but phylogenetic analyses based on cytochrome *b* data indicated that it is actually more closely related to *M. tricolor*. Discovery of this new taxon increases the number of *Myotis* species known from mainland Africa to 11 species, although patterns of molecular divergence suggest that cryptic species in the *Chrysopteron* clade remain to be described. This discovery also highlights the critical importance of the Nimba Mountains as a center of bat diversity and endemism in sub-Saharan Africa.

[1] Division of Vertebrate Zoology (Mammalogy), American Museum of Natural History, New York.
[2] Bat Conservation International, Austin, Texas.
[3] Department of Biological Sciences, Faculty of Sciences, University of Maroua, Maroua, Cameroon.
[4] Société des Mines de Fer de Guinée, Conakry, Guinea.
[5] Centre de Gestion de l'Environnement des Monts Nimba et Simandou/Ministère de l'Environnement, des Eaux et Forêts, Conakry, Guinea.
[6] Guinée Ecologie, Dixinn, Conakry, Guinea.
[7] Max Planck Institute of Molecular Cell Biology and Genetics, Dresden, Germany.
[8] Department Ecology and Evolutionary Biology, University of California, Santa Cruz.

 ISSN 0003-0082

INTRODUCTION

The genus *Myotis* is the most speciose genus of bats with over 120 extant species and a range that covers most of the world (Simmons, 2005; Simmons and Cirranello, 2020). *Myotis* bats are primarily insectivorous and range from tiny species that weigh only a few grams (e.g., *Myotis elegans*, 3–5 g; Reid, 2009) to quite large species (e.g., *Myotis chinensis*, 30–40 g; Francis, 2001), and have color patterns that range from brown or black to brightly colored yellow or orange, including some dichromatic taxa with particolored orange and black wings (e.g., *Myotis welwitschii*; Monadjem et al., 2010). Members of the genus are recognized by a combination of traits including ears that are longer than they are wide, a lanceolate tragus, a simple narial region with nostrils that open anterolaterally and not dorsally, a dental formula of I2/3, C1/1, P3/3, M3/3 = 38 (although some species lack p3 and P3), a single-rooted p3 that is somewhat smaller than p2, myotodont lower molars (although a few species are seminyctalodont), lower molars that have a relatively deep talonid basin, well-developed entocristid, and lack a lingual cingulid, a relatively high-crowned lower canine with well-developed mesial and distolingual shelves, a tall, daggerlike upper canine with a distinct lingual ridge, anterior upper premolars that are reduced in size compared to the P4, which is simple with rounded labial shelf, and an M1 and M2 with a distally open protofossa and lacking a paraconule and metaloph, and having a hypocone that is either small or absent (Findley, 1972; Koopman, 1994; Ruedi et al., 2015; Gunnell et al., 2017). Many species are cryptic and difficult to distinguish from similar congeners, and more than 20 new species have been described or elevated from synonymy in the last decade (Simmons, 2005; Simmons and Cirranello, 2020).

Only 11 species of *Myotis* are currently known from continental Africa, and only eight of these occur in tropical sub-Saharan regions, suggesting that new and/or cryptic species of *Myotis* likely remain to be discovered given the vast size and diverse habitats of the African continent (Patterson et al., 2019; Simmons and Cirranello, 2020). A recent study of genetic variation among and within populations of African *Myotis* by Patterson et al. (2019) found evidence of strong geographic structure within two species (*M. tricolor* and *M. welwitschii*) suggesting possible cryptic species in these complexes. As with many African bat taxa, sampling effort has been very uneven, especially in tropical areas, and large sampling gaps remain for all *Myotis* species (Patterson et al., 2019).

The Nimba Mountains are an isolated mountain range in West Africa that straddles the borders of Guinea, Liberia, and Côte d'Ivoire (fig. 1). With peaks rising between 1600–1750 m above sea level, the mountain range is surrounded by lowland habitats and occupies a transition zone between the tropical forest zone and moist woodlands. The Nimba Mountains support exceptional biodiversity including a diverse bat fauna that includes several threatened and endangered species (Brosett, 2003; Denys et al., 2013; Monadjem et al., 2016). In January and February 2018, and in March 2019, we conducted field surveys to assess the species diversity and distribution patterns of subterranean roosting bats in the northern (Guinean) portion of the Nimba Mountains. Surveys were carried out in the Mining Concession and Perimeter, managed by Société des Mines de Fer de Guinée S.A (SMFG), as well as in the adjacent World Heritage Site and surrounding lowlands, as part of SMFG's environmental and social impact

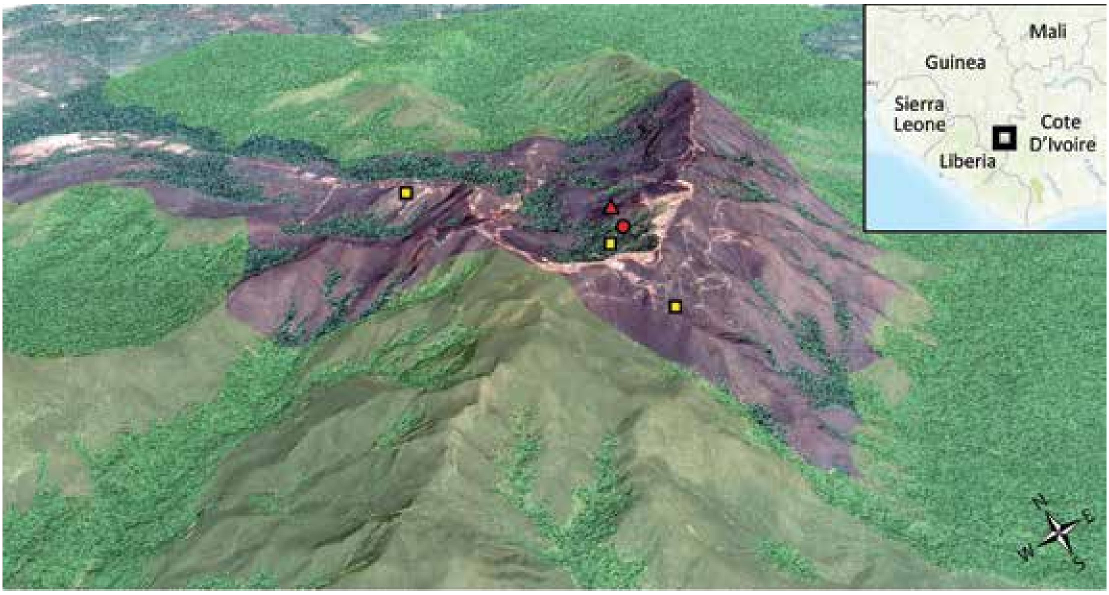

FIGURE 1. Relief map with satellite imagery overlaid showing the capture locations of the *Myotis nimbaensis* holotype (red triangle: captured 26 January 2018; red circle: collected 2 February 2018) and other sites where this species was likely detected with acoustic monitoring at entrances of underground sites (yellow squares). The mining concession footprint is shown as the unshaded area within the Nimba Mountains Strict Nature Reserve and Mount Nimba World Heritage Site (identical boundaries) that are overlaid by light green shading. Dominant habitat types are visible as different textures from the satellite imagery showing how gallery forests occur along steep canyons surrounded by savanna at higher elevations. Roads and trails in the mining concession are also visible as light brown features. Location of the Nimba Mountains in relation to Guinea, Liberia and Côte d'Ivoire is shown in the inset.

assessment for the Nimba Iron Ore Project. As part of this work, we captured two individuals of a spectacular dichromatic orange and black species clearly belonging to *Myotis* but that did not fit the diagnosis of any previously described species in the genus. We analyzed morphological, morphometric, echolocation, and molecular data, and herein describe these individuals as representing a new species of *Myotis* (subgenus *Chrysopteron*).

Genetic diversity and species limits of bats in the monophyletic subgenus *Chrysopteron* (= "Ethiopian Clade" of Stadelmann et al., 2004, and "Clade V" of Ruedi et al., 2013, 2015) were recently reviewed by Csorba et al. (2014) and Patterson et al. (2019). *Chrysopteron* as defined by Csorba et al. (2014) is the only traditional subgenus of *Myotis* currently validated by molecular systematics (Csorba et al., 2014; Patterson et al., 2019; Morales et al., 2019). This taxon, which is diagnosed morphologically by reddish or yellowish dorsal fur with a cottony or wooly texture, is distributed from Africa and Madagascar to the Mediterranean region, across India and southern Asia to China, Taiwan, Korea, the Philippines, Malaysia, and Indonesia (Csorba et al., 2014). *Myotis* (*Chrysopteron)* currently contains 14 species: *Myotis anjouanensis, M. bartelsi, M. bocagii*, *M. emarginatus*, *M. formosus*, *M. goudoti*, *M. hermani*, *M. morrisi*, *M. rufoniger*, *M. rufopictus*, *M. scotti*, *M. tricolor*, *M. weberi*, and *M. welwitschii* (Csorba et al., 2014; Patterson et al., 2019).

FIGURE 2. Photographs of roosting and surrounding habitats at the type locality in the Guinean Nimba Mountains. **A,** Entrance of Kaiser Adit 1. **B,** Entrance of Kaiser Adit 3 with harp trap placed for bat capture. **C,** Ecotone of savanna and gallery forest habitats at the headwaters of the Zié river viewable from where bats were captured at adit entrances.

MATERIALS AND METHODS

We surveyed subterranean habitats (abandoned mine adits and natural caves) by placing harp traps (a two-bank 4.2 m^2 harp trap [manufactured by Austbat] or a "cave catcher" 0.9 m^2 harp trap [Bat Conservation and Management]) at entrances at least 30 minutes before sunset (fig. 2). Harp traps were checked a maximum of every 10–15 minutes for the presence of bats for two to three hours after sunset and removed after bat emergence activity had subsided. Captured bats were placed in individual cloth bags and processed to identify species, sex, age, and reproductive status prior to release at place of capture following standard methods as described in Kunz and Parsons (2009). We collected standard field measurements (forearm length, tibia length, hind-foot length, tail length, ear length, tragus length, body length, and mass) and consulted *Mammals of Africa*, volume 4 (Hedgehogs, Shrews and Bats; Happold and Happold, 2013) to identify species. We collected tissue samples for DNA analysis using a 3 mm biopsy punch from the wing membrane and stored in desiccant. Echolocation calls were recorded upon release for echolocating bat species using a Pettersson M500 full-spectrum bat detector (Pettersson Elektronik) at a sampling rate of 500 kHz. Files were saved as uncompressed ".wav" format and analyzed using BatSound v.4.1 (Pettersson Elektronik: FFT size 1024, Hanning window) to determine the following parameters for each pulse: duration (D), maximum frequency (FMAX), minimum frequency (FMIN), peak frequency (PF), and interpulse interval (IPI). D, FMAX, FMIN, and IPI were measured from spectrograms, and PF from power spectrum.

A male bat captured and released on 26 January 2018 at Kaiser Adit 3 could not be identified using keys for the bats of Africa. Due to the likelihood that this individual represented an unknown species of *Myotis*, we resurveyed two adjacent adits (Kaiser Adit 1 and Kaiser Adit 3) on 2 February 2018 and collected two individuals (one male, one female) emerging from Kaiser Adit 1 to confirm and describe the species. The collected specimens included the male bat originally captured and released on 26 January 2018, identifiable by the 3 mm hole in its wing membrane from tissue sampling.

We employed analyses of mitochondrial cytochrome *b* gene sequences as well as standard morphological comparisons in our evaluation of the new taxon. The specimens examined and tissues used for this study (appendices 1 and 2) belong to the following collections:

AMNH American Museum of Natural History, New York
BMNH Natural History Museum, London
FMNH Field Museum of Natural History, Chicago
USNM National Museum of Natural History, Smithsonian Institution, Washington, DC

Molecular Analyses

Our analysis was designed to cover all the major lineages previously recognized in the subgenus *Chrysopteron* to allow placement of our new species in phylogenetic context. We downloaded GenBank sequences of *Myotis* compiled or originally published by Csorba et al. (2014) and were given early access to sequence data subsequently published in Patterson et al. (2019); see appendix 2. Data for an outgroup, *Submyotodon latirostris*, were also obtained from GenBank (appendix 2). Genomic DNA from the new species of *Myotis* was extracted at CIBIO-InBIO, University of Porto, Portugal, using Qiagen DNeasy kits (Qiagen, Crawley, UK) and stored at -20° C. Mitochondrial cytochrome *b* (cyt *b*) gene was amplified by polymerase chain reaction (PCR) using the primers MOLCIT-F (5′-AATGACAT-GAAAAATCACCGTTGT-3′; Ibáñez et al., 2006) and MVZ16-R (5′-AAATAGGAARTATCAYTCTGGTTTRAT-3′; Smith and Patton, 1993). PCR's were performed in a 10 μL volume, which included 1 μL of DNA extract, 0.4 μL of each primer (10 μM*)*, 5 μL of Qiagen Master Mix, and double-distilled water was added until final volume was reached. Reactions were performed under the following conditions: 95° C for 15 min; 40 cycles of 95° C for 30 s, 50° C for 45 s, 72° C for 1 min; 60° C for 10 min, and DNA sequencing performed on an ABI3700 DNA sequencer (Applied Biosystems).

Sequences were aligned using Geneious Prime v.2020.0.2 and edges of incomplete sequences were trimmed to reduce missing data. The final alignment included 102 individuals with 634 BP and 277 variables sites. Models of sequence evolution were explored in jModel test v.2.1.10 (Darriba et al., 2012) and likelihood scores calculated using PhyML v.3.0 (Guindon et al., 2010). The model that best fits the data, TrN+I+G (Tamura and Nei, 1993) was identified using the Akaike Information Criterion (wAIC = 0.9915). Phylogenetic inferences were performed using two approaches. First, we used a Bayesian approach as implemented in BEAST v.2.6.0 (Bouckaert et al., 2014). A Yule prior was used with a uniform distribution. Two independent chains were run, each for 50 million steps sampled every 5000, and a burn-in equivalent to 25%. Convergence was assessed using effective sampling size in Tracer v.1.7.1 (Rambaut et al., 2018). Trees from the posterior distribution were summarized using a maximum clade credibility tree using mean node heights and a burning equivalent to 25% as implemented in Tree Annotator v.2.6.0 (Drummond and Rambaut, 2007). Second, we use a maximum likelihood (ML) approach as implemented in RAxML v.8 (Stamatakis, 2014). The best scoring ML tree was estimated using 20 replicates. Nodal support was calculated by 100 bootstrap replicates. Finally, the percentage of genetic divergence among species of the subgenus *Chrysopteron* was calculated using Nei's dA index (Nei and Kumar, 2000) as implemented in strataG v.2.4.905 (Archer et al., 2017). Only taxa with more than two samples were included in the analysis.

Morphological Analyses

We examined 34 specimens of adult *Myotis* (15 males, 16 females, 3 of unknown sex; appendix 1) as well as literature descriptions of all *Chrysopteron* species, and evaluated external and osteological characters including but not restricted to those discussed by Hill and Morris

(1971), Smithers (1983), Koopman (1994), Taylor (2000), Monadjem et al. (2010), and Csorba et al. (2014). Dental homology nomenclature for premolars follows that of Csorba et al. (2014): 1st upper premolar (P2), 2nd or middle upper premolar (P3); 3rd upper premolar (P4), 1st lower premolar (p2), 2nd or middle lower premolar (p3), and 3rd lower premolar (p4). All measurements reported herein are from adult individuals with closed epiphyses. The first five measurements listed below were taken from skin labels or other records made by the original collector unless otherwise noted; all other measurements were taken by us using digital calipers and were recorded to the nearest 0.01 mm. Linear measurements are given in millimeters (mm), and weights are reported in grams (g). Descriptive statistics (mean and observed range) were calculated for all samples. Measurements are defined as follows:

Mass (M): Body weight in grams.

Total length (TL): Distance from the tip of the snout to the tip of the last caudal vertebra.

Length of tail (LT): Measured from the point of dorsal flexure of the tail with the sacrum to the tip of the last caudal vertebra.

Hind-foot length (HF): Measured from the anterior edge of the base of the calcar to the tip of the claw of the longest toe.

Ear length (Ear): Measured from the ear notch to the fleshy tip of the pinna.

Forearm length (FA): Distance from the elbow (tip of the olecranon process) to the wrist (including the carpals). This measurement is made with the wing at least partially folded.

Greatest length of skull (GLS): Distance from the posteriormost point on the occiput to the anteriormost point on the premaxilla (excluding the incisors).

Condyloincisive length (CIL): Distance between a line connecting the posteriormost margins of the occipital condyles and the anteriormost point on the upper incisors.

Condylobasal length (CBL): Distance between a line connecting the posteriormost margins of the occipital condyles and the anteriormost point on the skull not including the upper incisors.

Postorbital breadth (POB): Breadth across the narrowest portion of the postorbital region.

Braincase breadth (BB): Greatest breadth of the globular part of the braincase, excluding mastoid and paraoccipital processes.

Mastoid breadth (MB): Greatest breadth across the mastoid processes.

Zygomatic hreadth (ZB): Greatest breadth across the zygomatic processes.

Maxillary toothrow length (MTRL): Distance from the anteriormost surface of the upper canine to the posteriormost surface of the crown of M3.

Breadth across molars (BM): Greatest breadth across the outer margins of the upper molar teeth.

Breadth across canines (BC): Greatest breadth across the outer margins of the upper canines.

SYSTEMATICS

Family Vespertilionidae Gray, 1821

Subfamily Myotinae Tate 1942

Genus *Myotis* Kaup, 1829

Subgenus *Chrysopteron* Jentink, 1910

Myotis nimbaensis**,** new species

Nimba Myotis

Figures 3–8

HOLOTYPE: AMNH 279589, an adult male captured and released on 26 January 2018 at Kaiser Adit 3 and then collected on 2 February 2018 by Jon Flanders and Eric Moïse Bakwo Fils at Kaiser Adit 1 (fig. 2), Nimba Mountains, Guinea (N07.66499, W008.37223), field number BCIGU133. The specimen was preserved whole in formalin and stored in ethanol, and the skull was subsequently extracted and cleaned. A 3 mm wing biopsy tissue sample was collected and stored in desiccant before the DNA was extracted at CIBIO-InBIO, University of Porto, Portugal.

PARATYPE: AMNH 279590, an adult female collected at the same time and place as the holotype, field number BCIGU132. Like the holotype, the paratype was preserved in formalin and stored in ethanol after a 3 mm wing biopsy tissue sample was collected and stored in desiccant before the DNA was extracted. The skull was subsequently extracted and cleaned.

OTHER RECORDS: In addition to the captures of the holotype and paratype, we recorded echolocation calls from the male holotype on 26 January 2018. Once its distinctive call parameters were identified, we searched for its echolocation call signature in sound files recorded at the entrances of 10 mine adits between 2018–2019, including the type locality, within the Nimba Mountains' Mining Concession in Guinea (fig. 1), using Song Meter SM4BAT acoustic detectors (Wildlife Acoustics). Echolocation calls closely matching those recorded from the release calls of the holotype were detected at the entrances of a total of five mine adits (fig. 1) with seasonal variation between sites and the highest activity rates recorded at the type locality. While the Nimba Mountains support an exceptionally diverse bat fauna, this is the first *Myotis* species observed using the adits and only the second *Myotis* species to be recorded across the whole mountain range (Monadjem et al., 2016). Details of call frequency and structure, as well as comparisons with calls of congeneric species, are provided below in the section entitled Echolocation Calls.

DISTRIBUTION: Known only from the type locality and vicinity in the Guinean Nimba Mountains.

ETYMOLOGY: *Myotis nimbaensis* ("from Nimba") is named in recognition of the mountain range in which it was discovered. As an epithet referring to a place, *nimbaensis* is spelled the same way whether applied in combination with either a masculine or a feminine genus name. Woodman (1993) argued that *Myotis* should be considered feminine in gender, but Pritchard

(1994) disagreed. Both of these authors overlooked a 1958 ruling by the International Commission on Zoological Nomenclature that fixed the gender of *Myotis* as masculine and placed the name as such on the Official List of Generic Names in Zoology (International Commission on Zoological Nomenclature, 1958). So in this case, *nimbaensis* is masculine.

Diagnosis and Description: *Myotis nimbaensis* is diagnosed by a combination of the following characteristics: large size (FA 52.4–55.2 mm, mass 15.5–17.0 g; table 1) with females apparently somewhat larger than males; dorsal fur bright orange with strongly tricolored hairs (basal 1/3 of hair shaft black, middle 1/3 of shaft creamy white, distal 1/3 and tip bright orange to coppery red); ventral fur paler than dorsal fur, tricolored on belly (black base, buff-colored shaft that grades to orange at tip) grading to bicolored (lacking black base) on the sides near the wing membranes; ruff of brighter fur present around neck; pointed face with pale skin covered with orange fur, skin clearly visible through the fur around eye, mouth, and on rostrum; no black spots present on face; pinna with a rounded tip, relatively long and reaching beyond tip of nose when laid forward; pinna with strong distal emargination; skin of pinna pale orange brown becoming slightly darker near the tip, no rim of black around ear; tragus lanceolate, slightly less than half the length of the pinna; thumb brown; wing membranes strongly dichromatic black and orange, with plagiopatagium and dactylopatagium mostly black with narrow bands of orange along the metacarpals, phalanges, and across the membrane behind the forearm and upper arm; black pigmentation extends medially nearly to body and posteromedially to tibia; membrane between metacarpals I and II pale orange; propatagium pale orange; uropatagium orangish brown with orange fur on the proximal 1/3 of the dorsal surface and pale cream-colored fur on proximal 1/5 of ventral surface; no black spots on patagia; no conspicuous gland present in plagiopatagium behind humerus; pale ventral fur extends onto proximal plagiopatagium in narrow strip along body, does not extend past knee; relatively small foot with length approximately 2/5 of tibia length; foot and toes brown, with sparse long brown hairs on the dorsal surface of each toe; wing membrane essentially naked except close to the body, where it has a sparse covering of cream colored hairs on the ventral surface; wing membrane attaches to foot at base of first toe; calcar long, more than twice the length of the hind foot, runs approximately 2/3 of the length of the uropatagium border; skull large for *Myotis* (GLS = 19.48–19.73 mm; CIL = 18.92–18.93 mm; CBL = 18.31–18.81 mm) with globular braincase, well-defined sloping forehead, and elongated supraorbital region all contributing to the appearance of a clearly defined and elongate rostrum; rostrum with shallow medial depression in nasal region; sagittal crest moderately well developed in both sexes; lambdoid crest weakly developed in both sexes; dental formula I2/3, C1/1, P 3/3, M3/3 = 38; I1 and I2 each with a well-developed posterior cusp; upper canine robust, crown height approximately 2× that of P4, basal area (as seen in occlusal view) roughly equal to that of P4; anterior two premolars (P2 and P3) much smaller than last premolar (P4); P3 with less than half the basal area of P2 and shifted lingually to be partly excluded from the toothrow although still visible in lateral view; P4 large, sharply pointed, taller than M1; lower incisors each with 4 main cusps; i3 with distal accessory cuspules; p3 relatively large, approximately three quarters the basal area of p2, and fully in line in toothrow, not shifted lingually; lower molars myotodont.

FIGURE 3. Portrait of *Myotis nimbaensis* (AMNH 279589, holotype). **A,** View of right side of upper body and head showing the pale ventral fur and bright orange fur on the head and the ruff around the neck; also note the brown color of the thumb. **B,** Anterior view of the left ear showing the pale orange-brown color of the pinna, strong distal emargination, and rounded pinna tip. **C,** Anterior view of right ear showing the ridges in the pinna and the relative length of the lanceolate tragus, which is slightly less than half the length of the pinna. **D,** Close-up view of the right side of the head showing the pale skin visible through the fur around eye, mouth, and on the rostrum; also note the strongly tricolored fur on the top of the head.

Comparisons: External and craniodental measurements for *Myotis nimbaensis* and other congeneric African species with which it might be confused are provided in table 1. In addition to *M. nimbaensis*, three other large *Myotis* (subgenus *Chrysopteron*) species with orange dorsal fur occur in Africa: *M. tricolor*, *M. welwitschii*, and *M. morrisi*. Descriptions and measurements of these species can be found in Hill and Morris (1971), Hill et al. (1988), Taylor (2000), and Monadjem et al. (2010); the latter work also includes color photographs and echolocation call spectrograms.

Myotis nimbaensis can be easily distinguished from *M. morrisi* on the basis of size, with *M. morrisi* being smaller in all external and craniodental dimensions (table 1). The ventral pelage of *M. morrisi* is also different—rather than being tricolored as in *M. nimbaensis*, *M. morrisi* has unicolored dull cream white ventral fur that is tinged a faint brown on the flanks and chin. The skull and dentition of *M. morrisi* is very similar to that of *M. nimbaensis* although the braincase of *M. morrisi* is somewhat more globular and lacks the sagittal crest seen in *M. nimbaensis*.

TABLE 1. Comparative measurements of *Myotis nimbaensis*, n. sp., and related African species. Mass (M) is in grams, all other measurements are in mm; see Materials and Methods for descriptions of measurements. Summary statistics (mean, observed range in parentheses, and sample size) are given for samples that include multiple individuals.

	M. nimbaensis		*M. morrisi*	*M. tricolor*		*M. welwitschii*	
	Male[a]	Female[b]	Female[c]	Males[d]	Females[e]	Male[f]	Female[g]
M	15.5	17.0	8.0	10.4 (8.5–12.5) 5	10.25 (9.0–12.0) 4	–	–
TL	111.6	116.3	93.0	108.0 (102.0–116.0) 10	112.4 (104.0–120.0) 10	–	120.0
LT	41.4	46.8	45.0	49.1 (45.0–53.0) 10	52.9 (46.0–61.0) 10	–	55.0
HF	12.0	13.0	10.0	10.3 (9.0–12.0) 9	11.7 (10.0–13.0) 9	–	10.0
Ear	19.5	20.0	16.0	17.8 (15.0–19.0) 10	17.8 (16.0–19.0) 9	–	21.0
FA	52.4	55.2	47.0	48.7 (46.0–50.6) 9	50.3 (48.3–51.6) 10	58.6	55.3
GLS	19.48	19.73	17.01	17.72 (17.11–18.76) 11	18.05 (16.97–18.63) 13	18.94	19.12
CIL	18.93	18.92	16.93	16.82 (15.92–18.07) 10	17.15 (16.09–18.04) 12	18.90	18.60
CBL	18.39	18.81	15.90	16.36 (15.55–17.43) 9	16.70 (15.38–17.94) 13	17.87	17.72
POB	4.75	4.65	3.94	4.38 (3.94–4.64) 12	4.28 (3.91–4.46) 12	5.11	4.84
BB	9.11	9.13	8.07	8.58 (7.84–8.94) 12	8.63 (8.42–8.94) 13	9.33	8.92
MB	9.80	9.86	8.62	9.14 (8.87–9.56) 12	9.31 (9.07–9.58) 12	10.22	9.62
ZB	12.85	12.97	10.60	11.53 (10.84–12.49) 8	11.62 (11.17–12.27) 12	13.14	–
MTRL	7.76	7.89	6.80	6.95 (6.60–7.68) 12	6.96 (6.58–7.37) 12	7.82	7.62
BM	8.20	8.26	6.42	7.34 (7.01–7.79) 12	7.44 (7.09–7.80) 13	7.91	8.24
BC	5.44	5.40	4.15	7.71 (4.44–5.13) 10	4.78 (4.57–5.08) 11	–	5.40

[a] Holotype, AMNH 279589. HF and Ear measurements were taken after preservation. Additional measurement taken in the field: Tibia 22.35, Tragus 9.61.
[b] Paratype, AMNH 279590. HF and Ear measurements were taken after preservation. Additional measurement taken in the field: Tibia 23.28, Tragus 10.62.
[c] Holotype, BMNH 70.488.
[d] AMNH 232029, 232030, 257053; BMNH 14.5.4.2, 64.172, 75.2550, 75.2551, 75.2554, 87.1082; USNM 317927, 317928, 342645, 351061.
[e] AMNH 146789, 257358; BMNH 40.740, 40.741, 75.2549, 75.2552, 75.2553, 75.2555; USNM 292066, 238099, 342634, 242644, 351060.
[f] BMNH 22.12.17.75.
[g] BMNH 22.12.17.76.


A
B
C
D
E

Myotis nimbaensis is similar in size and general coloration to the widespread species *M. welwitschii*, but these taxa can be easily distinguished because *M. nimbaensis* completely lacks the prominent black spots seen on the face and patagia of *M. welwitschii* (figs. 3–6). Color of the pinnae is also different—bright orange to coppery red with a black edge in *M. welwitschii* compared to pale orange brown with no black edge in *M. nimbaensis*. The thumb in *M. welwitschii* is bright orange whereas it is brown in *M. nimbaensis*. Both species are strongly dichromatic with black wing membranes and orange along the digits and forearm, but pigmentation of the plagiopatagium near the body and hind legs is different in the two species. *Myotis welwitschii* has a broad band of orange along the side of the body that extends anteriorly past the elbow to run along the forearm and posteriorly to the ankle, so black pigmentation is limited to the more distal and posterior portions of the plagiopatagium. In contrast, the orange is much less extensive and the black is more extensive in *M. nimbaensis*; the black pigmentation approaches the body wall, extending anteriorly into the plagiopatagium behind the humerus and posteriorly to the tibia in *M. nimbaensis*, so there is no broad band of orange along the body in that species. The uropatagium in *M. welwitschii* is also bright orange whereas it is darker and more brownish in *M. nimbaensis*. There are additional differences in features of the dorsal and ventral pelage—the dorsal fur in *M. welwitschii* is bicolored (black at base and otherwise coppery red) rather than being tricolored as in *M. nimbaensis*, and *M. welwitschii* has unicolored ventral pelage (whitish tinged with coppery red) rather than the distinctive tricolored ventral fur in seen in *M. nimbaensis*.

Craniodental measurements (table 1) suggest overall similarity of *M. nimbaensis* with *M. welwitschii;* small differences in a few dimensions are not interpretable given the small sample sizes. Both species have lambdoidal crests that are weakly developed but clearly visible, and moderately well-developed sagittal crests in both sexes. The dentition of *M. welwitschii* includes two very small anterior upper premolars that are both included in the toothrow; P3 is smaller than P2, but P3 is not displaced lingually as it is in *M. nimbaensis*.

Myotis tricolor is a widespread species that shows considerable morphometric variation across its range (Koopman, 1989, 1994; Taylor, 2000; Monadjem et al., 2010). *Myotis nimbaensis* is roughly equivalent in overall size (e.g., forearm length and body mass) to the largest individuals of *M. tricolor* reported in the literature, although none of the specimens of *M. tricolor* that we measured were as large as *M. nimbaensis*. The only known specimen of *M. tricolor* from West Africa—a male from Liberia referred to that species by Koopman (1989)—is much smaller than *M. nimbaensis*, having a forearm length of 46.0 mm compared to 52.4 mm for the male paratype

FIGURE 4. Fur color and banding in *Myotis nimbaensis* (AMNH 279589, holotype). **A,** View of the dorsal fur showing the overall bright orange coloration; creamy white bands on the hairs proximal to the bright orange fur tips are visible on the lower right near the leg where the fur has been somewhat disturbed. **B,** Close-up of dorsal fur over the lower back showing tricolored fur in a spot on the center left where the fur has been slightly teased apart; where the fur is undisturbed, the banding of individual hairs is not visible. **C,** dorsal fur over lower back clearly showing the tricolored banding in an area where the fur has been separated by blowing. **D,** Ventral fur over torso showing overall paler coloration than dorsal fur, and tricolored banding of the hairs with less orange at the tips. **E,** Ventral fur over left side of the thorax showing bicolored banding (lack of a black basal band) near the wing membrane.

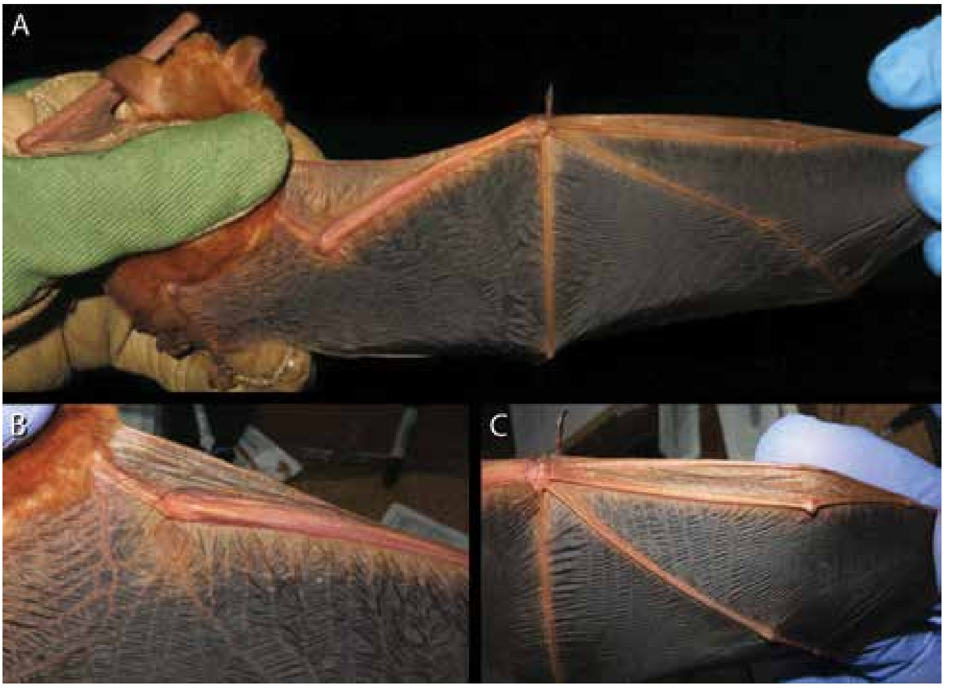

FIGURE 5. Coloration of the wing membranes in *Myotis nimbaensis* (AMNH 279589, holotype). **A,** Dorsal surface of the wing showing the dichromatic black and orange skin coloration. The plagiopatagium and dactylopagial membranes are mostly black with thin orange bands along the metacarpals, phalanges, and forearm; the black pigmentation also extends nearly to the body wall in the area between the forearm and the hind leg. The propatagium is pale orange. **B,** Dorsal surface of the anterior and proximal portion of the wing showing the patterning of the black pigmentation near the body. **C,** Dorsal surface of the distal wing showing the brown thumb and orange (not black) pigmentation of the membrane between digits II and III.

of *M. nimbaensis*. The pelage of *M. tricolor* is similar to that of *M. nimbaensis*, and *M. tricolor* similarly lacks black spots on the face or tail membrane. However, these species can be distinguished easily based on coloration of the wing membranes: *M. tricolor* has wings that are dark brown rather than the distinctive dichromatic orange and black wings seen in *M. nimbaensis*. The pinnae of *M. tricolor* are dark brown compared with the pale orange brown seen in *M. nimbaensis*, and the emargination is more proximally located (nearly at the midpoint of the lateral edge of the pinna) in *M. tricolor* compared to the clearly distal location of the emargination in *M. nimbaensis*. The uropatagium of *M. tricolor* is also darker brown (rather than orange brown as in *M. nimbaensis*) and has a dense covering of coppery red fur proximately (more sparse in *M. nimbaensis*). In terms of craniodental features, *M. nimbaensis* has a greater condylobasal length (18.9 mm for both sexes) than seen in *M. tricolor* (15.9–18.5 mm including data from table 1 and Monadjem et al., 2010). Although our comparative sample of *M. tricolor* was not large, we found that most other craniodental measurements similarly appear to distinguish *M. nimbaensis* and *M. tricolor*, with *M. nimbaensis* the larger of the two species.

Sagittal crest development in *Myotis tricolor* is variable, with females typically lacking any sagittal crest development. In contrast, both male and female *M. nimbaensis* have well-devel-

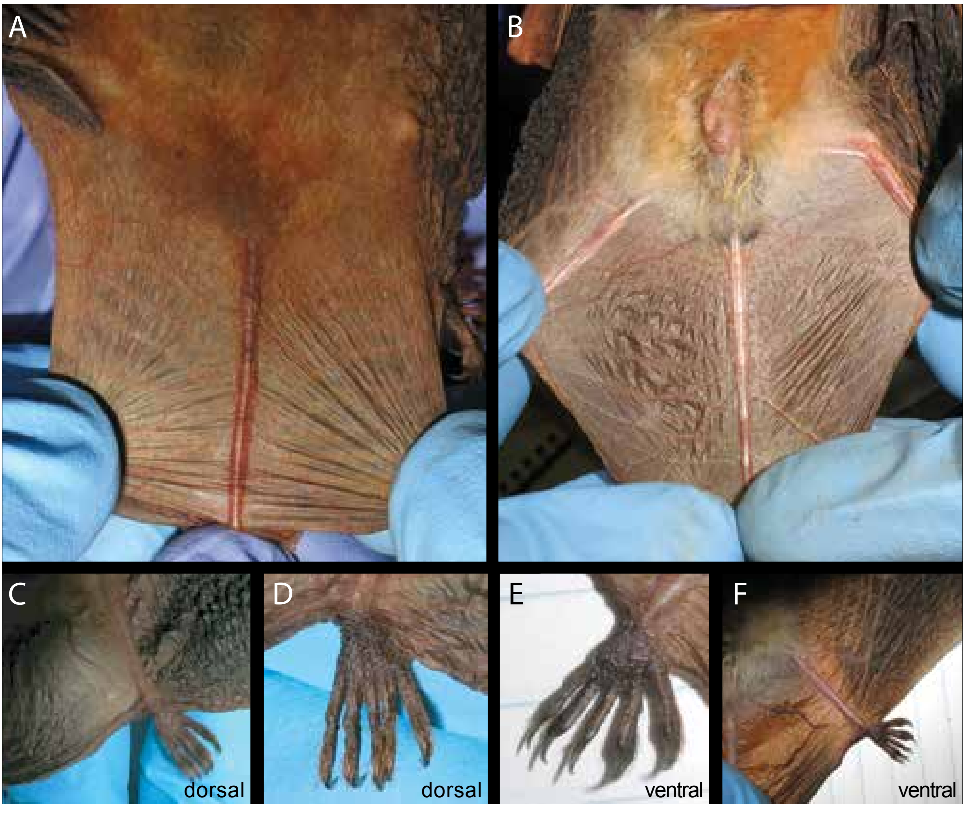

FIGURE 6. Uropatagium, foot, calcar, and flight membrane attachments in *Myotis nimbaensis* (AMNH 279589, holotype). **A,** Dorsal side of the uropatagium showing orangish brown skin with orange fur on the proximal 1/3 of the surface of the membrane. **B,** Ventral side of uropatagium showing pale cream-colored fur on proximal 1/5 of ventral membrane surface; this fur continues across the femur onto the proximal plagiopatagium in a narrow strip that does not extend past the knee. **C,** Dorsal view of distal leg, foot, calcar, and associated flight membranes. Note that the wing membrane (on right of the foot) attaches to the foot at the base of the first toe, and the calcar (on the left of the foot) is more than twice the length of the hind foot. **D,** Close-up of the dorsal surface of the foot showing sparse, long brown hairs on each toe. **E,** Close-up of the ventral side of foot and toes showing dark brown coloration. **F,** Ventral view of the hind leg and foot showing the relatively small foot size (foot length = 2/5 of tibia length) and the patterning of black membrane pigmentation near the leg and foot.

oped sagittal crests (though again, our sample size is small). Upper premolars in *M. tricolor* are somewhat variable, but P3 is always less than half the basal area of P2 and is always shifted lingually as in *M. nimbaensis*. However, in many individuals the reduction in P3 is greater than in *M. nimbaensis*, and this tooth is completely excluded from the toothrow (only partly excluded in *M. nimbaensis*). The p3 of *M. tricolor* is one half to two thirds the basal area of p2, and p3 is sometimes displaced lingually from the toothrow, compared to a slightly larger p3 that is at least three quarters the size of p2 and which is not displaced in *M. nimbaensis*.

Another orange *Myotis* species from Africa is *M. bocagii*, which occurs across much of tropical Africa and is broadly sympatric with *M. tricolor* and *M. welwitschii* (Monadjem and Jacobs, 2017a; Patterson, 2019). *Myotis bocagii* can be easily distinguished from *M. nimbaensis*

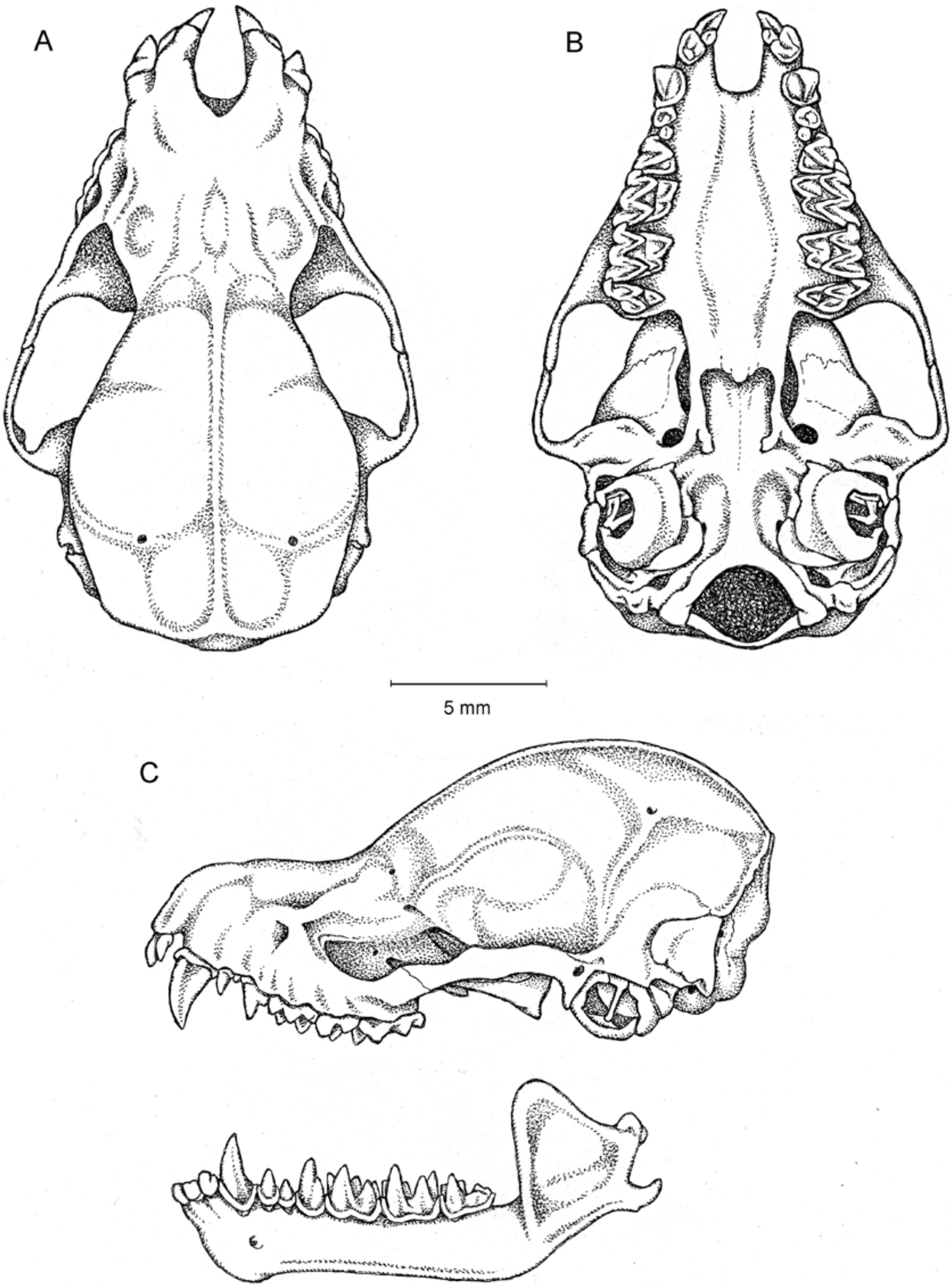

FIGURE 7. Skull and jaws of *Myotis nimbaensis* (AMNH 279589, holotype): **A,** dorsal view of skull; **B,** ventral view of skull; **C,** lateral view of skull and lower jaws. (Drawings by Patricia J. Wynne.)

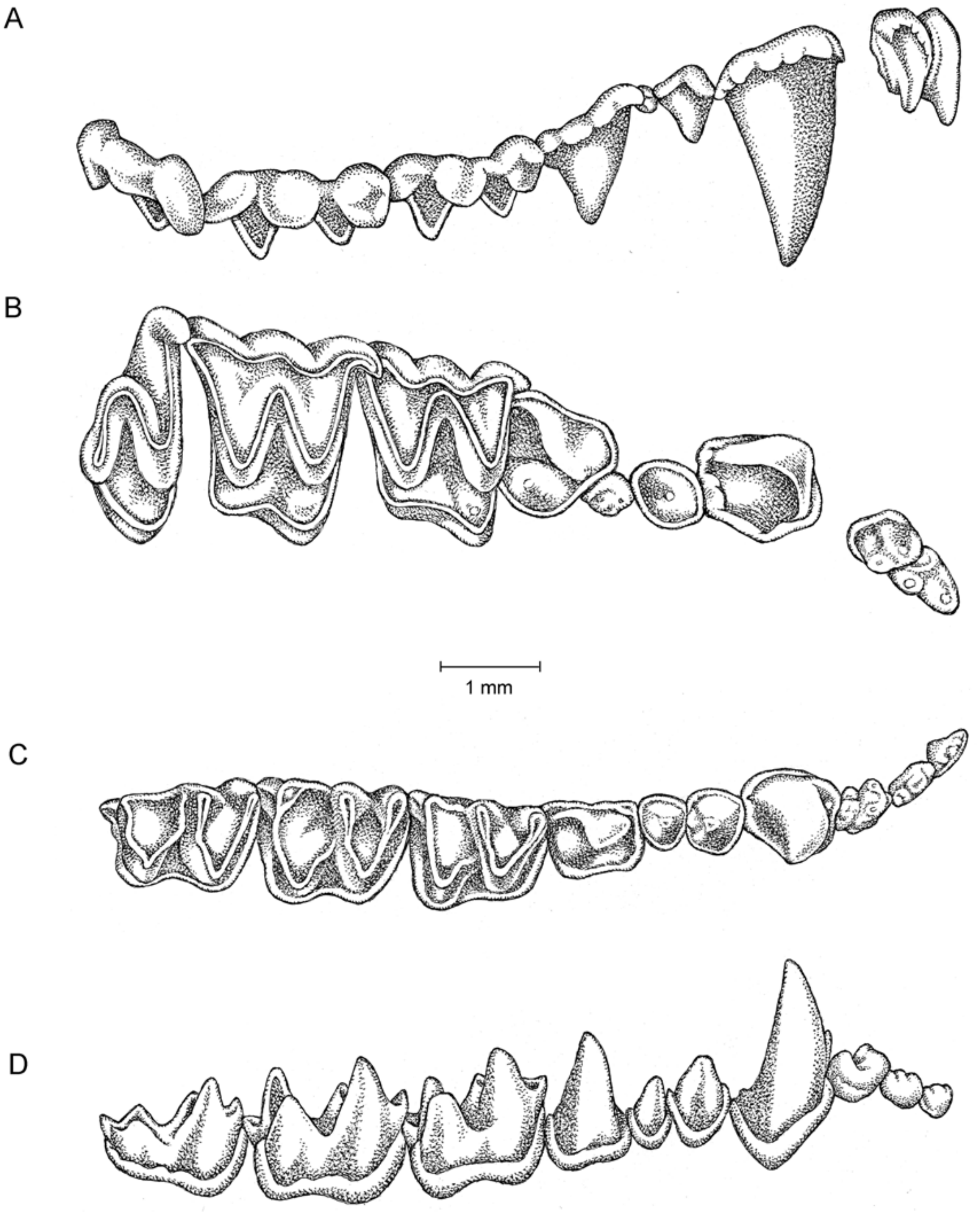

FIGURE 8. Dentition of *Myotis nimbaensis* (AMNH 279589, holotype): **A,** lateral view of upper toothrow; **B,** occlusal view of upper toothrow; **C,** occlusal view of lower toothrow; **D,** lateral view of lower toothrow. (Drawings by Patricia J. Wynne.)

based on its dark brown wings and considerably smaller size in all dimensions (e.g., FA = 36.0–40.5 mm; mass = 6.0–9.0 g.; CBL = 13.0–15.0 mm; CIL = 14.0–15.2 mm; Koopman, 1994; Monadjem et al., 2010).

Myotis (subgenus *Chrysopteron*) species with yellow or orange dorsal fur and dichromatic orange and black wings are not limited to Africa, but also occur in Asia. At least six Asian species (*M. bartelsi, M. formosus, M. hermani, M. rufoniger, M. rufopictus,* and *M. weberi*) exhibit color patterns with dichromatic wing pigmentation superficially similar to that of *M. nimbaensis* (Csorba et al., 2014). Csorba et al. (2014) gave diagnoses and measurements of these species that provide a basis for distinguishing them from *M. nimbaensis*. These authors recognized two pelage and skin color patterns among the Asian species: a "*rufoniger* type" and a "*formosus* type." Species exhibiting "*rufoniger* type" morphology include *M. bartelsi, M. hermani, M. rufoniger,* and *M. weberi*. These species can be distinguished from *M. nimbaensis* based on darker dorsal pelage that has four bands of color (individual dorsal hairs black basally, pale yellow distally, then darkening to deep red before terminating in a black tip; Csorba et al., 2014) rather than the bright orange tricolored dorsal fur of *M. nimbaensis*. Species with "*rufoniger* type" coloration are also considerably darker ventrally than *M. nimbaensis*, having hairs with a black base, followed by either a pale yellowish section that progressively darkens distally to deep red, or are otherwise entirely deep red (Csorba et al., 2014). The ear is also edged with black in *rufoniger*-type species (Csorba et al., 2014), a trait lacking in *M. nimbaensis* (or any other African species of *Chrysopteron*). The thumb and underside of hind foot are entirely black in species with "*rufoniger* type" coloration (Csorba et al., 2014) but not in *M. nimbaensis*, which has an orange-brown thumb and a brown foot. *Myotis rufoniger* has flight membranes with a broad band of red that extends from the ankle to the forearm along the side of the body, and black pigmentation is limited to the more distal and posterior portions of the plagiopatagium (Bhak et al., 2017). In contrast, the black pigment is more extensive in *M. nimbaensis*, extending much closer to the body including reaching the tibia and into the membrane behind the humerus, and the pale portions of the wings are more orange than red.

Members of the *Myotis rufoniger* group vary somewhat in size, but they are all large bats roughly comparable in size to *M. nimbaensis*. Measured forearm lengths of *M. rufoniger* (FA = 45.0–56.0; Csorba et al., 2014) overlap with those of *M. nimbaensis*, but cranial dimensions of *M. rufoniger* (e.g., GLS = 16.98–19.24 mm; ZB = 10.04–12.24 mm) do not overlap, with *M. nimbaensis* being the slightly larger species. Dental morphology is also somewhat different; *M. rufoniger* has a P3 that is roughly two thirds the size of P2 and which is usually in line with the other check teeth (rarely displaced lingually; Csorba et al., 2014), compared with *M. nimbaensis*, in which P3 is less than half the size of P2 and is lingually displaced. Considerable overlap in most dimensions exists between *M. nimbaensis* and *M. weberi* (FA = 49.7–53.5 mm; GLS = 19.15–19.72 mm; ZB = 12.37–12.67 mm; Csorba et al., 2014). However, *M. weberi* as described by Csorba et al. (2014) can be distinguished by having a relatively short upper canine that is only about 1.5× the height of P4 (C height is ~2× height of P4 in *M. nimbaensis*) and a p3 that is no more than half the basal area of p2 (p3 is at least three quarters the basal area of p2 in *M. nimbaensis*).

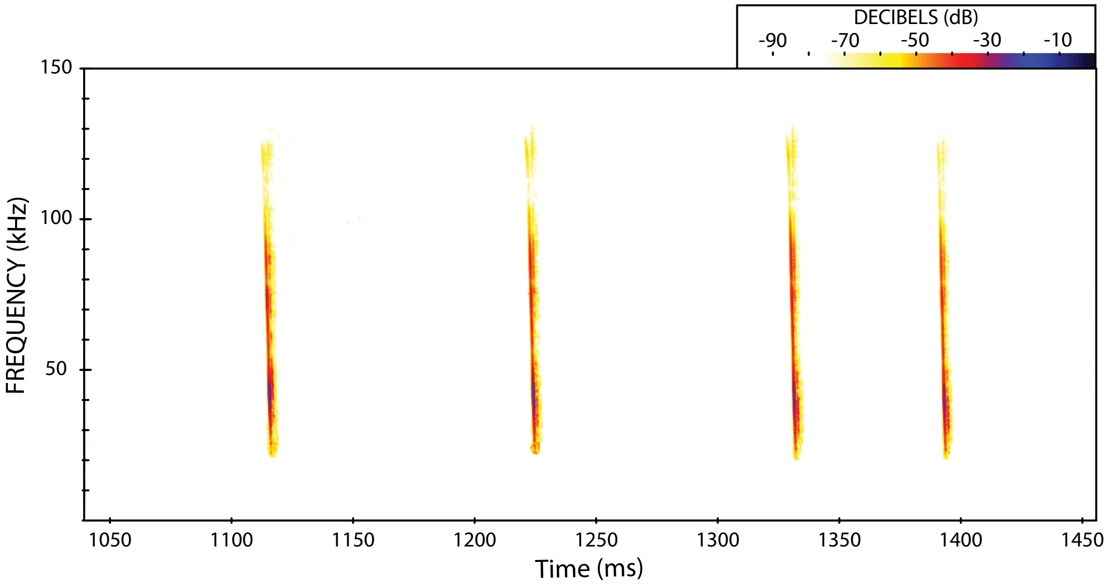

FIGURE 9. Spectrogram of echolocation calls emitted by the holotype *Myotis nimbaensis* upon initial release (FFT size 1024, Hanning window; sampling rate of 500 kHz). Color scale represents amplitude of sound in decibels (dB).

In contrast to *Myotis rufoniger* and *M. weberi*, both *M. bartelsi* (FA = 53.4 mm; GLS = 20.42 mm; ZB = 13.41 mm) and *M. hermani* (FA = 56.0–60.0 mm; GLS = 20.10–21.77 mm; ZB = 13.4–14.10 mm) are somewhat larger than *M. nimbaensis* in most dimensions (Csorba et al., 2014). As described by Csorba et al. (2014), *M. bartelsi* can be distinguished by having strong lambdoid crests (weakly developed in *M. nimbaensis*) and a P3 that is fully out of line with the rest of the toothrow and not visible in lateral view (partially out of line and visible in lateral view in *M. nimbaensis*). The forehead is also less clearly developed and strongly sloped in *M. bartelsi* compared to *M. nimbaensis*, and the rostrum appears somewhat shorter in *M. bartelsi* in lateral view. *Myotis hermani* as described by Csorba et al. (2014) can be distinguished by its overall very robust skull and exceptionally well-developed sagittal and lambdoid crests (more weakly developed in *M. nimbaensis*), very large upper canine with a basal area exceeding that of P4 (basal areas of C and P4 subequal in *M. nimbaensis*), minute P3 less than one quarter the size of P2 (P3 only slightly less than one half the size of P2 in *M. nimbaensis*), P3 fully out of line with the rest of the toothrow and not visible in lateral view (only partially out of line and visible in lateral view in *M. nimbaensis*), p3 with half the basal area of p2 (p3 is at least three quarters the basal area of p2 in *M. nimbaensis*), and p3 partly lingually displaced out of the toothrow (p3 fully in toothrow in *M. nimbaensis*).

Asian *Myotis* (subgenus *Chrysopteron*) species exhibiting "*formosus* type" external morphology are *M. formosus* and *M. rufopictus* (Csorba et al., 2014). These species can be distinguished from *M. nimbaensis* based on pelage color and banding. The dorsal fur of *formosus*-type species has individual hairs that have a very narrow brown base and are pale yellow distally for 80–100% of their length, or grade into a brown tip, with banding sometimes not evident as the color changes gradually (Csorba et al., 2014). Overall, the general aspect of the dorsal fur in *M. formosus* and *M. rufopictus* is pale yellow-brown (Csorba et al., 2014). This pattern is very different from the distinctly banded tricolored orange fur of *M. nimbaensis*. Ventral fur of *M. formosus* and *M. rufopictus* is either bicolored light yellow with a narrow brown base, or unicolored light yellow (Csorba et al., 2014), again quite different from tricolored buff to orange ventral fur of *M. nimbaensis*. The ear is faintly edged with black in the *formosus*-type species (Csorba et al., 2014) but not in *M. nimbaensis*. As in *M. rufoniger*, the dark pigment in the wing membranes of *M. formosus* is limited to more distal and posterior portions of the plagiopatagium and does not extend to the tibia and membranes next to the body as it does in *M. nimbaensis*.

Measurements and craniodental features also distinguish *Myotis nimbaensis* from *M. formosus* and *M. rufopictus*. In terms of measurements, *M. nimbaensis* is only trivially different or falls within the range of variation in measurements reported for *M. formosus* (FA = 45.5–53.0 mm; GLS = 17.91–19.45 mm; ZB = 11.76–12.94 mm; Csorba et al., 2014). However, *M. formosus* as described by Csorba et al. (2014) can be distinguished based on having a sagittal crest that is missing or only very weakly developed (moderately well developed in *M. nimbaensis*), P3 that is not visible in lateral view of the skull (visible in *M. nimbaensis*), and a p3 with half the basal area of p2 (p3 is at least three quarters the basal area of p2 in *M. nimbaensis*). In addition, the skull of *M. formosus* lacks an expanded supraorbital region and appears to have a shorter rostrum than *M. nimbaensis* when seen in lateral view. *Myotis rufopictus* (FA = 51.0–52.5 mm; GLS = 18.2 mm; ZB = 11.17; Csorba et al., 2014) appears slightly smaller than *M. nimbaensis,* but both species are known from very few specimens, so the value of this observation is questionable. As described by Csorba et al. (2014), the skull profile of *M. rufopictus* ascends almost evenly with no frontal depression (i.e., no clearly defined break between rostrum and sloping forehead as seen in *M. nimbaensis*). Like *Myotis formosus, M. rufopictus* additionally lacks an expanded supraorbital region and it appears to have a shorter rostrum than *M. nimbaensis* when seen in lateral view. Morphology of P3 in *M. rufopictus* is unknown, but p3 is a very small tooth less than one quarter the basal area of p2 and displaced lingually halfway out of the line of toothrow (p3 at least three quarters the area p2 and not displaced in *M. nimbaensis*).

Echolocation calls: Based on the echolocation calls recorded on the release of the holotype (n = 22), *Myotis nimbaensis* emits a broad bandwidth (84.1 ± 13.1 kHz; FMAX: 104 kHz, FMIN: 20 kHz) steep frequency-modulated pulse with a peak frequency of 42.5 kHz (± 4.2 kHz), an average call duration of 3.5 ms (± 0.3 ms), and an interpulse interval of 113 ms (± 5.3 ms; fig. 9). In comparison, echolocation calls of *Myotis welwitschii* have a lower peak frequency (34 kHz), shorter bandwidth (28.3 kHz) and shorter duration (2.4 ms; Schoeman and Jacobs, 2008: Monadjem et al., 2010: Collen, 2012). While there may be geographic variation in call parameters between East African and Southern African *Myotis tricolor* populations, calls recorded from Southern Africa have a slightly higher peak frequency (47.8±3.1 kHz) but are shorter in bandwidth (46±23.9 kHz) and duration (3.3±0.6 ms; Schoeman and Jacobs, 2008: Monadjem et al., 2010). Echolocation calls of *Myotis morrisi* are unknown. *Myotis bocagii*, the other known Myotis species found on the Nimba Mountains, have calls with a similar peak frequency (41–43 kHz) but are shorter in bandwidth (36 kHz) and duration (2–2.8 kHz) (Schoeman and Waddington, 2011; Collen, 2012; Monadjem et al., 2017a).

Molecular Analyses: Molecular analyses of mitochondrial cytochrome *b* sequences from selected specimens (appendix 2) support recognition of *Myotis nimbaensis* as a distinct species (table 2, figs. 10 and 11). Our analyses recovered well-supported clades consistent with results of Csorba et al. (2014) and Patterson et al. (2019), and in this context *Myotis nimbaensis* was found to represent a distinct lineage that nests within the subgenus *Chrysopteron* as sister to the *M. tricolor* complex (the clade consisting of *M. tricolor* 1, 2, and 3 of Patterson et al., 2019). Monophyly of *Myotis nimbaensis*, the *M. tricolor* complex, and a clade consisting of these two lineages was highly supported (>95% bootstrap). *Myotis nimbaensis* is 5.18% different than *M. tricolor* 1, 5.43% from *M. tricolor* 2, and 5.08% than *M. tricolor* 3 (table 2).

Natural History: The type locality habitat of *Myotis nimbaensis* occurs at the ecotone of high-altitude grassland, montane savanna, and gallery forest habitats of the Nimba Mountains around 1400 m elevation (fig. 1). As far as is known, the preferred (or exclusive) roosting habitat for this species is subterranean features. The two individuals that we captured were emerging from day roosting in an abandoned mine adit (fig. 1), and echolocation calls similar to the release calls of *Myotis nimbaensis* recorded at other nearby adits, apparently confirming association of *M. nimbaensis* with these underground structures. *Myotis nimbaensis* coroosts with other subterranean roosting bats and was detected at mine adits that house colonies of several hundred *Rhinolophus guineensis* and *Hipposideros lamottei*, the latter a bat species endemic to the Nimba Mountains (Monadjem et al., 2013).

Foraging habitat for *Myotis nimbaensis* is unknown, but the six mine adits where *M. nimbaensis* echolocation calls were recorded occur in similar ecotone habitats at the interface of high-elevation grassland, montane savanna, and gallery forests along headwaters of the Zié, Gouan, and Zougué rivers in the northern Guinean Nimba Mountains.

DISCUSSION

Discovery of a new large *Myotis* in western Africa is perhaps not surprising given the complexity of habitat types and relative lack of exploratory studies across much of the region. Moreover, considering the large gaps in the ranges of many known species, it seems likely that many populations remain unsampled, and other new species will be discovered in future years. Little is known about the habits of *Myotis nimbaensis* other than characteristics of the type locality and roosting habits at the type locality. However, this information provides a basis for comparisons with other species in the subgenus *Chrysopteron*.

Habitat use and Roosting habits in African *Chrysopteron*: Comparisons of the natural history of *M. nimbaensis* with that of similar African congeners is hindered by lack of information about these unusual bats. The best known of these is *Myotis tricolor*, a taxon known from Ethiopia, Liberia, and the Democratic Republic of Congo south to South Africa (Simmons, 2005; Monadjem and Jacobs, 2017b; Patterson et al., 2019). *Myotis tricolor* as

TABLE 2. Percentage of sequence divergence among species of the subgenus *Chrysopteron* based on Nei's dA index and 634 bp of mitochondrial cytochrome *b*. Values of divergence between *Myotis nimbaensis* and closely related species are shown in bold. *Myotis tricolor* and *M. welwitchii* groups are clades identified by Patterson et al. (2019) as follows: *Myotis tricolor* 1 includes populations from Kenya and Uganda; *M. tricolor* 2 and *M. tricolor* 3 are both from South Africa; *M. welwitschii* 1 is from Kenya and Uganda; and *M. welwitschii* 2 includes populations from Tanzania, Malawi, and South Africa.

	M. bocagii	***M. formosus***	***M. goudoti***	***M. nimbaensis***	***M. rufoniger***	***M. tricolor* 1**	***M. tricolor* 2**	***M. tricolor* 3**	***M. welwitschii* 1**
M. formosus	17.04								
M. goudoti	13.04	14.47							
M. nimbaensis	**12.35**	**12.47**	**11.61**						
M. rufoniger	14.89	16.54	15.24	**11.76**					
M. tricolor 1	14.19	13.32	13.77	**5.18**	13.42				
M. tricolor 2	14.63	14.10	13.54	**5.43**	13.05	4.06			
M. tricolor 3	13.90	12.71	12.66	**5.08**	13.15	3.71	3.12		
M. welwitschii 1	14.21	16.27	14.29	**12.85**	11.80	13.90	13.72	13.09	
M. welwitschii 2	14.75	16.45	14.86	**12.91**	12.18	13.39	13.53	13.12	4.08

currently recognized apparently represents a species complex (see Patterson et al., 2019; figs. 10, 11), and most of what is known about these bats is based on observations of South African populations. The *M. tricolor* complex occurs primarily in savanna woodland in mountainous areas, penetrating into drier, more open terrain in the southern part of their range (Smithers, 1983; Taylor, 2000; Monadjem et al., 2010). These bats apparently roost exclusively underground in caves and mines, where they are gregarious and roost in tight clusters (Taylor, 1998, 2000; Monadjem et al., 2010). Average group size in South Africa is apparently a few dozen individuals, but *M. tricolor* may congregate in groups as large as 1400 to 2000 individuals (McDonald et al., 1990; Taylor, 1998, 2000; Monadjem et al., 2010). *Myotis tricolor* may share roosts with *Miniopterus* species (Taylor, 1998, 2000). *Myotis tricolor* is known to be migratory in parts of South Africa, flying hundreds of kilometers between summer maternity caves and winter hibernation caves (Taylor, 1998, 2000). Smithers (1983) and Monadjem et al. (2010) speculated that the occurrence of *M. tricolor* is probably governed more by the availability of caves and mine adits than by the vegetational associations or terrain in which they are found. In this respect *M. nimbaensis* may be similar. Despite numerous bat surveys in the Nimba region (summarized by Monadjem et al., 2016), the only place this species has been found is in association with mine adits in the Mining Concession area in the Guinean Nimba Mountains. We recorded echolocation activity at sunset and sunrise at mine adit entrances, indicating *M. nimbaensis* regularly roosts in abandoned adits. Colony size of *M. nimbaensis* may be small, as small as a few to single individuals, based on typically very low levels of echolocation activity at mine entrances where the species was detected. With known occurrence at only a single locality at 1400 m of elevation, *M. nimbaensis* is likely much more of a habitat specialist than are members of the *M. tricolor* complex, which appear to have a broader geographic range.

Myotis welwitschii (known from Ethiopia and the Democratic Republic of Congo south to South Africa; Simmons, 2005; Monadjem et al., 2017b; Patterson et al., 2019) is thought to be more of a habitat specialist tied to paramontane areas covered by woodland or woodland-forest mosaic vegetation; it has been captured also in riverine coastal forest adjacent to sugar cane fields and open thornveld (Smithers, 1983; Taylor, 1991, 1998; 2000; Fahr and Ebigbo, 2003). *Myotis welwitschii* is thought to be a solitary species (Taylor, 1991, 2000; Ratcliffe, 2002). Roosting habits of *M. welwitschii* are poorly known, but this species has been found roosting in vegetation including low bushes and shrubs, trees, furled banana leaves, and a single individual has also been captured in a cave (Smithers and Wilson, 1979; Rautenbach, 1982; Smithers, 1983; Skinner and Smithers, 1990; Taylor, 1998, 2000; Monadjem et al., 2010). At least two specimens of *M. welwitschii* were collected hanging in the open during the day, and in at least one case the bat was mistaken for a dead leaf before being revealed as a roosting bat (Taylor, 2000). It is possible that the unusual fur color and dichromatic wings of this species help to provide camouflage under such conditions.

Myotis morrisi is a rare species known only from Ethiopia and Nigeria (Hill and Morris, 1971; Hill et al., 1988; Simmons, 2005), a range that suggests either that many populations remain unsampled or that it represents a species complex. The holotype of *M. morrisi* was collected in 1968 on the Great Abbai Expedition in Ethiopia, where it was captured over the Blue Nile about 1 m above the water (Hill and Morris, 1971). The surrounding habitat was mostly maize fields and thick brush (Hill and Morris, 1971). The Nigerian specimen of *M. morrisi* was captured by mistnet in the Sudan savannah in a region of short grass and acacia bush, with some silk cotton trees, near the River Benue (Hill et al., 1988). Nothing is known about the roosting habits of this species.

Foraging habits: Three ecomorphs of *Myotis* are generally recognized: aerial netters (also called aerial hawkers), gleaners, and trawlers (Findley, 1972; Koopman, 1994; Ruedi and Mayer, 2001; Morales et al., 2019). Each of these is characterized by a suite of phenotypic traits involving ear length, skull shape, wing length and width, leg and foot length, and attachment site of the posterior plagiopatagium (Morales et al., 2019). Morales et al. (2019) used these traits to determine the ecomorph class for over 90 *Myotis* species, and they classified the majority of *Chrysopteron* species as gleaners including *Myotis welwitschii, M. tricolor, M. rufoniger, M. formosus, M. emarginatus,* and *M. goudoti*. *Myotis scotti* was classified as an aerial netter, and *M. bocagii* as a trawler (Morales et al., 2019). Given the morphological similarity of *Myotis nimbaensis* to *M. welwitschii*, *M. tricolor*, *M. rufoniger*, and *M. formosus*, we might expect that *M. nimbaensis* is also a gleaner. However, the usefulness of these categorizations for *Chrysopteron* species remains to be determined. Stoffberg and Jacobs (2004) tested the abilities of captive *Myotis tricolor* to catch prey presented in a variety of ways, and they found that while this species easily captured aerial prey, it did not glean. Those authors noted that *M. tricolor* has more pointed wings than many bats known to glean, and also varies from known gleaners in the genus *Myotis* (e.g., *M. lucifugus* and *M. septentrionalis*) in using short bandwidth echolocation calls that typically lack harmonics. In contrast, *M. septentrionalis* consistently produces two harmonics in addition to the dominant one, and *M. lucifugus* produces one harmonic in addition to the dominant harmonic (Stoffberg and Jacobs, 2004) effectively making the bandwidth of their calls even broader. While we did not detect any harmonics in the release calls of *M. nimbaensis,* we found that it produced broader bandwidth calls than those of *Myotis tricolor*. Although its relatively long call duration may suggest *M. nimbaensis* is not specialized for gleaning, it is similar to that of *Myotis lucifugus,* which is both an aerial hunter and gleaner (Ratcliffe and Dawson 2003).

Details of foraging habits and diet of African *Chrysopteron* are poorly known. Nothing is known of the diet of *M. morrisi,* and a description of *M. welwitschii* feeding on small beetles is based on fecal pellets from a single individual (Moratelli, 2019). Captive individuals apparently prefer soft-shelled insects (Happold and Happold, 2013). *Myotis welwitschii* has been observed entering houses at night while foraging (Skinner and Smithers, 1990; Taylor, 1998)

FIGURE 10. Maximum likelihood phylogenetic reconstruction of subgenus *Chrysopteron* using an alignment of 634 base pairs of mitochondrial gene cytochrome *b*. Colored circles at nodes represent support values as bootstrap percentage from maximum likelihood analyses. Support values lower than 50% at shallow nodes are not shown. Tip labels indicate GenBank accession number and locality. *Myotis tricolor* 1, 2, and 3 and *M. welwitschii* 1 and 2 are labeled following Patterson et al. (2019).

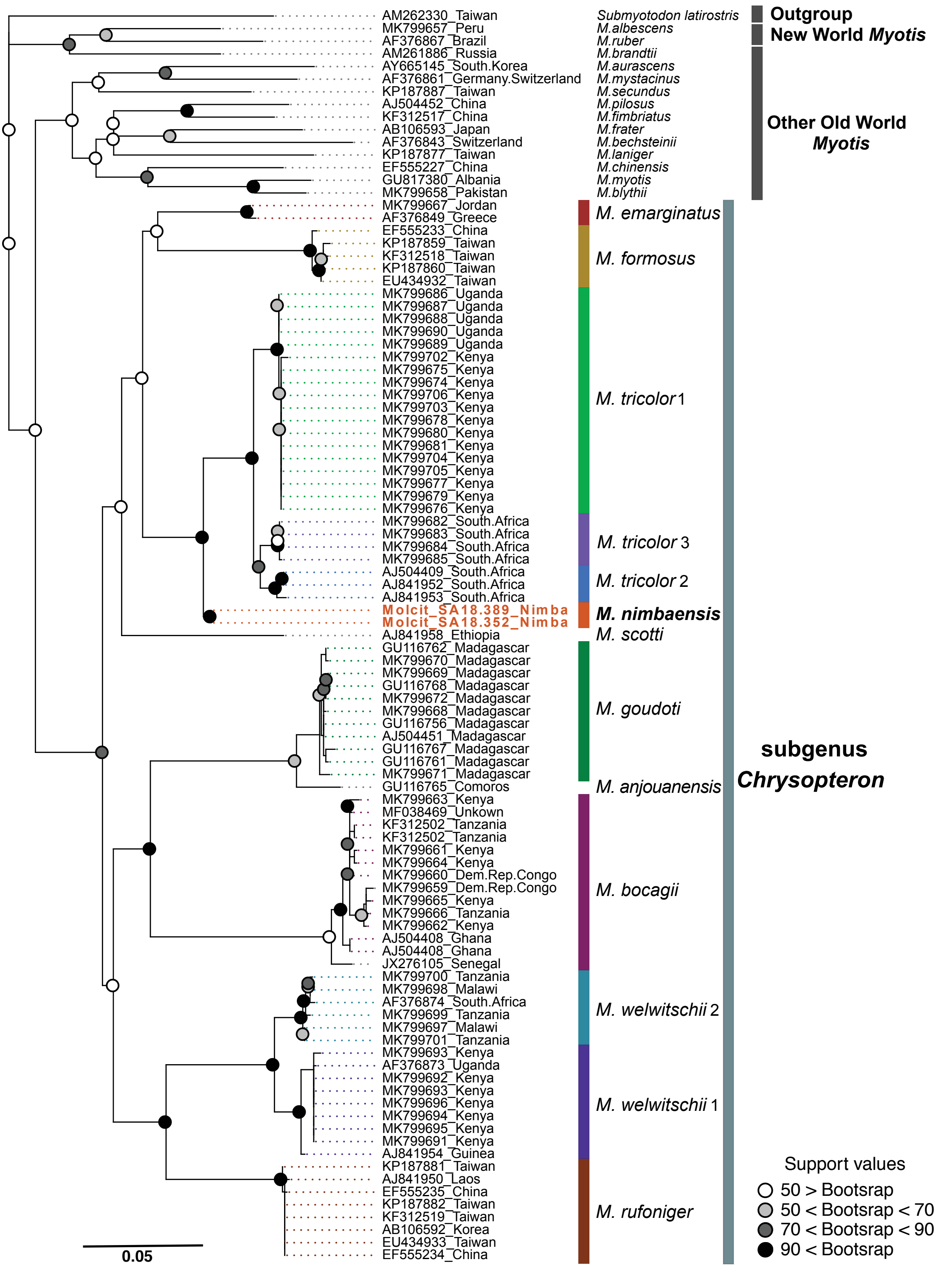

AM262330_Taiwan
MK799657_Peru
AF376867_Brazil
AM261886_Russia
AY665145_South.Korea
AF376861_Germany.Switzerland
KP187887_Taiwan
AJ504452_China
KF312517_China
AB106593_Japan
AF376843_Switzerland
KP187877_Taiwan
EF555227_China
GU817380_Albania
MK799658_Pakistan
MK799667_Jordan
AF376849_Greece
EF555233_China
KP187859_Taiwan
KF312518_Taiwan
KP187860_Taiwan
EU434932_Taiwan
MK799686_Uganda
MK799687_Uganda
MK799688_Uganda
MK799690_Uganda
MK799689_Uganda
MK799702_Kenya
MK799675_Kenya
MK799674_Kenya
MK799706_Kenya
MK799703_Kenya
MK799678_Kenya
MK799680_Kenya
MK799681_Kenya
MK799704_Kenya
MK799705_Kenya
MK799677_Kenya
MK799679_Kenya
MK799676_Kenya
MK799682_South.Africa
MK799683_South.Africa
MK799684_South.Africa
MK799685_South.Africa
AJ504409_South.Africa
AJ841952_South.Africa
AJ841953_South.Africa
Molcit_SA18.389_Nimba
Molcit_SA18.352_Nimba
AJ841958_Ethiopia
GU116762_Madagascar
MK799670_Madagascar
MK799669_Madagascar
GU116768_Madagascar
MK799672_Madagascar
MK799668_Madagascar
GU116756_Madagascar
AJ504451_Madagascar
GU116767_Madagascar
GU116761_Madagascar
MK799671_Madagascar
GU116765_Comoros
MK799663_Kenya
MF038469_Unkown
KF312502_Tanzania
KF312502_Tanzania
MK799661_Kenya
MK799664_Kenya
MK799660_Dem.Rep.Congo
MK799659_Dem.Rep.Congo
MK799665_Kenya
MK799666_Tanzania
MK799662_Kenya
AJ504408_Ghana
AJ504408_Ghana
JX276105_Senegal
MK799700_Tanzania
MK799698_Malawi
AF376874_South.Africa
MK799699_Tanzania
MK799697_Malawi
MK799701_Tanzania
MK799693_Kenya
AF376873_Uganda
MK799692_Kenya
MK799693_Kenya
MK799696_Kenya
MK799694_Kenya
MK799695_Kenya
MK799691_Kenya
AJ841954_Guinea
KP187881_Taiwan
AJ841950_Laos
EF555235_China
KP187882_Taiwan
KF312519_Taiwan
AB106592_Korea
EU434933_Taiwan
EF555234_China
0.05
Submyotodon latirostris
M.albescens
M.ruber
M.brandtii
M.aurascens
M.mystacinus
M.secundus
M.pilosus
M.fimbriatus
M.frater
M.bechsteinii
M.laniger
M.chinensis
M.myotis
M.blythii
M. emarginatus
M. formosus
M. tricolor 1
M. tricolor 3
M. tricolor 2
M. nimbaensis
M. scotti
M. goudoti
M. anjouanensis
M. bocagii
M. welwitschii 2
M. welwitschii 1
M. rufoniger
Outgroup
New World Myotis
Other Old World Myotis
subgenus Chrysopteron
Support values
50 > Bootsrap
50 < Bootsrap < 70
70 < Bootsrap < 90
90 < Bootsrap

but has been also been observed flying low over streams and a farm pool, suggesting that it may also forage by trawling over open water (Ratcliffe, 2002; Moratelli, 2019). *Myotis tricolor* in South Africa feeds primarily on hard-bodied prey with coleopterans making up the greatest proportion of the diet, followed by hemipterans (Stoffberg and Jacobs, 2004). There is no evidence that they feed on lepidopterans, and no insects or other arthropods that are potential substrate prey have been found in dietary analyses based on fecal samples (Stoffberg and Jacobs, 2004). The diet of *M. nimbaensis* remains unknown.

Phylogenetic relationships, biogeography, and evolution: Molecular phylogenies indicate that *Chrysopteron* split from other Old World *Myotis* early in the radiation of the genus (Stadelmann et al., 2004; Morales et al., 2019). Stadelmann et al. (2004) dated this split to the middle Miocene (~10–13 Mya), but a slightly older Miocene date (~16–18 Mya) was recently proposed using revised calibration points and a more extensive data set (Morales et al., 2019). Not surprisingly given the overlap of our data sets, our phylogenetic results echoed those of Csorba et al. (2014) and Patterson et al. (2019) in confirming monophyly of *Chrysopteron* with moderate support. Within this clade, each of the currently recognized species (sensu Csorba et al., 2014) was found to be distinct and, if represented by more than one sequence, monophyletic (figs. 10, 11). Although support values for some basal relationships with *Chrysopteron* were not high, some biogeographically and morphologically interesting clades were strongly supported in our analyses. Two dichromatic species from different continents, *Myotis rufoniger* (Asia) and the *M. welwitschii* complex (Africa) were found to be sister taxa, suggesting that they shared a dichromatic common ancestor. Rather than grouping with this clade, the two other dichromatic species, *M. nimbaensis* and *M. formosus*, group in different parts of the tree. *Myotis nimbaensis* is strongly supported as the sister taxon of the *M. tricolor* species complex, which does not have dichromatic coloring although both are from mainland Africa; *Myotis formosus* from Asia forms a weakly supported clade with nondichromatic *M. emarginatus* from the Mediterranean region. Another strongly supported clade within *Chrysopteron* is comprised of monochromatic species known only from Africa and nearby Indian Ocean islands (*Myotis bocagii*, *M. goudoti*, and *M. anjouanensis*). Although low support values limit the value of further interpretations, it seems clear that dichromatic coloration evolved at least twice and possibly three or four times in *Chrysopteron*, and that intercontinental dispersal events occurred at least twice in this subgenus although directionality of these events cannot be determined with any certainty given the data at hand. Additional data from genes capable of resolving more basal relationships within *Chrysopteron* will be necessary to fully resolve these questions.

The Nimba Mountains as a Center of Bat Diversity and Endemism: The Nimba Mountains are well known as a center of biodiversity and endemism (Brosset, 2003; Lamotte and Roy, 2003; Wieringa and Poorter, 2004; Sandberger et al., 2010; Denys and

FIGURE 11. Bayesian phylogenetic reconstruction of subgenus *Chrysopteron* using an alignment of 634 base pairs of mitochondrial gene cytochrome *b*. Colored circles at nodes represent support values as posterior probability from Bayesian analyses. Support values lower than 50% at shallow nodes are not shown. Tip labels indicate GenBank accession number and locality. *Myotis tricolor* 1, 2, and 3 and *M. welwitschii* 1 and 2 are labeled following Patterson et al. (2019).

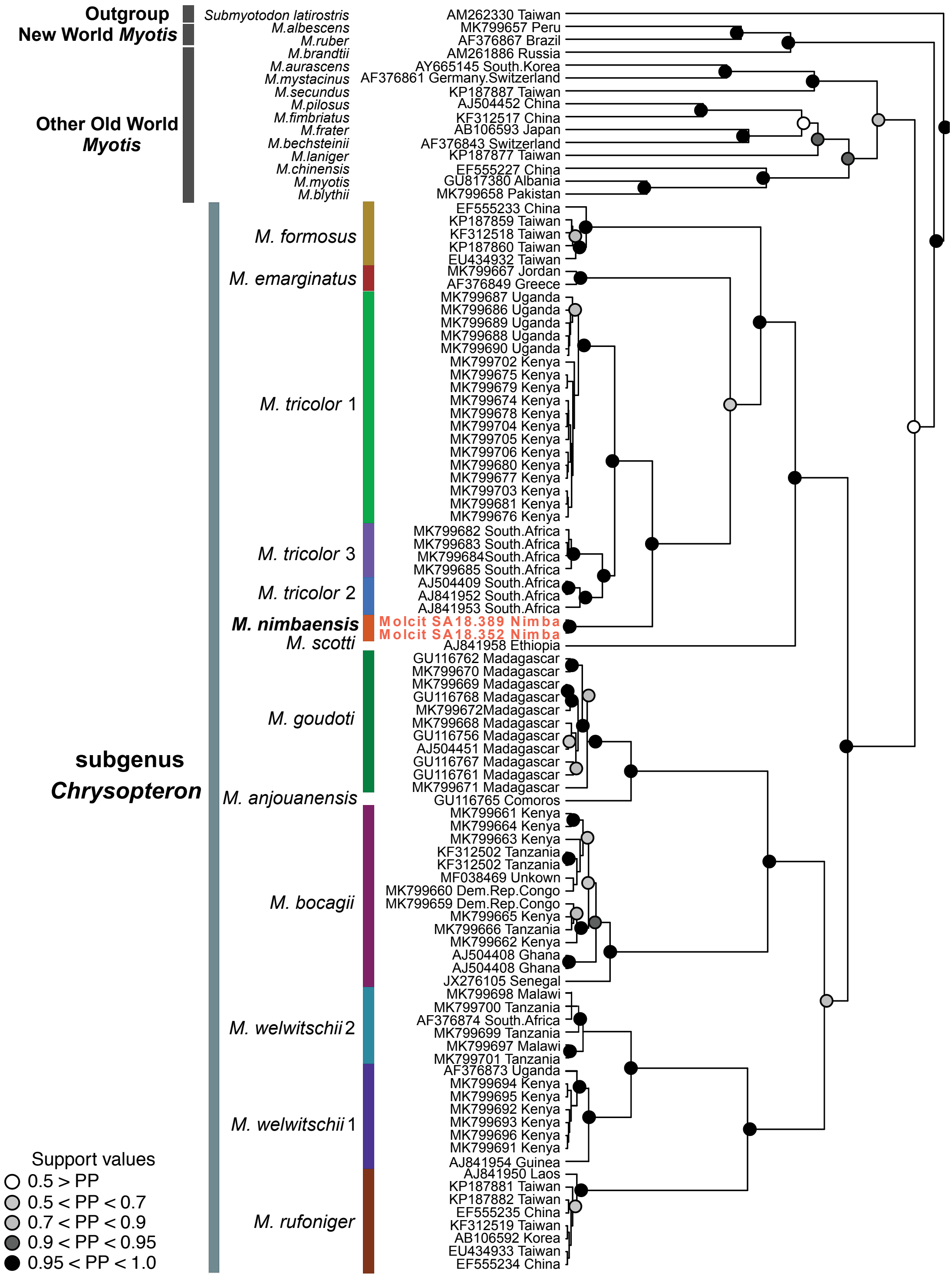

Outgroup
New World Myotis
Other Old World Myotis
subgenus Chrysopteron
Submyotodon latirostris
M.albescens
M.ruber
M.brandtii
M.aurascens
M.mystacinus
M.secundus
M.pilosus
M.fimbriatus
M.frater
M.bechsteinii
M.laniger
M.chinensis
M.myotis
M.blythii
M. formosus
M. emarginatus
M. tricolor 1
M. tricolor 3
M. tricolor 2
M. nimbaensis
M. scotti
M. goudoti
M. anjouanensis
M. bocagii
M. welwitschii 2
M. welwitschii 1
M. rufoniger
AM262330 Taiwan
MK799657 Peru
AF376867 Brazil
AM261886 Russia
AY665145 South.Korea
AF376861 Germany.Switzerland
KP187887 Taiwan
AJ504452 China
KF312517 China
AB106593 Japan
AF376843 Switzerland
KP187877 Taiwan
EF555227 China
GU817380 Albania
MK799658 Pakistan
EF555233 China
KP187859 Taiwan
KF312518 Taiwan
KP187860 Taiwan
EU434932 Taiwan
MK799667 Jordan
AF376849 Greece
MK799687 Uganda
MK799686 Uganda
MK799689 Uganda
MK799688 Uganda
MK799690 Uganda
MK799702 Kenya
MK799675 Kenya
MK799679 Kenya
MK799674 Kenya
MK799678 Kenya
MK799704 Kenya
MK799705 Kenya
MK799706 Kenya
MK799680 Kenya
MK799677 Kenya
MK799703 Kenya
MK799681 Kenya
MK799676 Kenya
MK799682 South.Africa
MK799683 South.Africa
MK799684South.Africa
MK799685 South.Africa
AJ504409 South.Africa
AJ841952 South.Africa
AJ841953 South.Africa
Molcit SA18.389 Nimba
Molcit SA18.352 Nimba
AJ841958 Ethiopia
GU116762 Madagascar
MK799670 Madagascar
MK799669 Madagascar
GU116768 Madagascar
MK799672Madagascar
MK799668 Madagascar
GU116756 Madagascar
AJ504451 Madagascar
GU116767 Madagascar
GU116761 Madagascar
MK799671 Madagascar
GU116765 Comoros
MK799661 Kenya
MK799664 Kenya
MK799663 Kenya
KF312502 Tanzania
KF312502 Tanzania
MF038469 Unkown
MK799660 Dem.Rep.Congo
MK799659 Dem.Rep.Congo
MK799665 Kenya
MK799666 Tanzania
MK799662 Kenya
AJ504408 Ghana
AJ504408 Ghana
JX276105 Senegal
MK799698 Malawi
MK799700 Tanzania
AF376874 South.Africa
MK799699 Tanzania
MK799697 Malawi
MK799701 Tanzania
AF376873 Uganda
MK799694 Kenya
MK799695 Kenya
MK799692 Kenya
MK799693 Kenya
MK799696 Kenya
MK799691 Kenya
AJ841954 Guinea
AJ841950 Laos
KP187881 Taiwan
KP187882 Taiwan
EF555235 China
KF312519 Taiwan
AB106592 Korea
EU434933 Taiwan
EF555234 China
Support values
0.5 > PP
0.5 < PP < 0.7
0.7 < PP < 0.9
0.9 < PP < 0.95
0.95 < PP < 1.0

Aniskine, 2012; Denys et al., 2013; Marshall and Hawthorne, 2013; Monadjem et al., 2013, 2016, 2019). As summarized by Monadjem et al. (2016), many surveys of the bats of the Nimba region have been conducted over the past several decades, with the majority of work done on the Liberian side of the mountain range. The discovery of *Myotis nimbaensis* brings the known number of bat species in the Nimba Mountains to 62 species (Monadjem et al., 2016, 2019). Five new species of bats have been described from the region in the last decade: *M. nimbaensis (this study)*, *Neoromicia roseveari* (Monadjem et al., 2013), *N. isabella* (Decher et al., 2015), *Parahypsugo happoldorum* (Hutterer et al., 2019), and *Miniopteris nimbae* (Monadjem et al., 2019). Two species are endemic to the mountain range (*Myotis nimbaensis* and *Hipposideros lamottei*) and two more are highly restricted regional highland endemics (*Hipposideros marisae* and *Rhinolophus ziama*; Monadjem et al., 2016). *Hipposideros marisae* is known only from highland regions of Guinea, Liberia, and Côte d'Ivoire (Fahr, 2013), and was observed by the authors in 2018 roosting in a small natural cave at 491 m in the buffer zone of the World Heritage Site in the Guinean Nimba Mountains (unpublished data). Similarly, *Rhinolophus ziama* is restricted to Guinea and Liberia and likely a specialist restricted to mountain habitats (Fahr et al., 2002; Simmons and Cirranello, 2020). Given this pattern, if *Myotis nimbaensis* has a range extending beyond the Nimba Mountains, we would expect it to similarly occur in highland regions elsewhere in Guinea, Liberia, and Côte d'Ivoire. Acoustic surveys of these areas would be a good way to determine if *M. nimbaensis* has a broader ranger or is an endemic restricted in range to only to the Nimba Mountains.

Two species coroosting in mine adits on the Nimba Mountains with *M. nimbaensis* are considered threatened by IUCN: *Rhinolophus guineensis* (IUCN status: Endangered) and *Hipposideros lamottei* (IUCN status: Critically Endangered) (Shapiro and Cooper-Bohannon, 2020; Mickleburgh et al., 2008). In addition, two other species occurring in the Nimba range that have been assessed by IUCN are considered threatened—*Hipposideros marisae* (IUCN status: Vulnerable) and *Rhinolophus ziama* (IUCN status: Endangered) (Monadjem et al. 2016). Including *Myotis nimbaensis*, 10 taxa—one sixth of the total bat species diversity of the Nimba Mountains—have yet to have their conservation status fully assessed by the IUCN. Although some of these lineages may be fairly widespread in West Africa, others will likely turn out to mirror the endemic *Hipposideros* and *Rhinolophus* of the area that are strictly endemic to a one or a few mountainous areas. *Myotis nimbaensis,* which may be limited by both underground roosting habits and affinity for habitat and vegetation combinations found only in the highlands, may well be one of these taxa. The striking color pattern of *M. nimbaensis* and its lack of black facial spots (spots highly characteristic of *M. welwitschii*, the only bat in West Africa that it superficially resembles) suggests that *M. nimbaensis* is unlikely to have been overlooked or misidentified in previous surveys in the region. It therefore seems very likely that it is an uncommon to rare endemic with a very small geographic range. In this context, we expect that *M. nimbaensis* will be classified as a critically endangered species when it is assessed by the IUCN based on having a known extent of occurrence less than 100 km^2 (IUCN 2012).

ACKNOWLEDGMENTS

The authors would like to thank Patrick Jules Atagana and Marcel Leno for their assistance during the 2018 field expedition to Nimba. We would also like to thank Darrin Lunde (USNM) and Roberto Portela Miguez (BMNH) for access to specimens needed for this project, and for kindly hosting N.B.S. during visits to their respective institutions. We also thank Bruce Patterson and Terry Demos (FMNH) for prepublication access to their data, and Bruce Patterson and Gabor Csorba for thoughtful reviews of the manuscript. A.E.M. was supported by a Gerstner Postdoctoral Fellowship from the American Museum of Natural History.

REFERENCES

Anwarali Khan, F.A., et al. 2010. Systematics of Malaysian woolly bats (Vespertilionidae: *Kerivoula*) inferred from mitochondrial, nuclear, karyotypic, and morphological data. Journal of Mammalogy, 91 (5): 1058–1072.

Archer, F.I., P.E. Adams, and B.B. Schneiders. 2017. strataG: an r package for manipulating, summarizing and analysing population genetic data. Molecular Ecology Resources 17 (1): 5–11.

Bhak, Y., et al. 2017. *Myotis rufoniger* genome sequence and analyses: *M. rufoniger*'s genomic feature and the decreasing effective population size of *Myotis* bats. PloS One 12 (7).

Bouckaert, R., et al. 2014. BEAST 2: A software platform for Bayesian evolutionary analysis. PLoS Computational Biology 10 (4). [doi: 10.1371/journal.pcbi.1003537]

Brosset, A. 2003. Les chiroptères du Mont Nimba. *In* M. Lamotte and R. Roy (editors), Le peuplement animal du Mont Nimba (Guinée, Côte d'Ivoire, Liberia): 687–693. Mémoires du Muséum National d'Histoire Naturelle 190, 724 pp.

Collen, A. 2012. The evolution of echolocation: a comparative approach. Ph.D. dissertation, Division of Biosciences, University College London, London, UK.

Csorba, G., et al. 2014. The reds and the yellows: a review of Asian *Chrysopteron* Jentink, 1910 (Chiroptera: Vespertilionidae: *Myotis*). Journal of Mammalogy 95 (4): 663–678.

Darriba, D., G.L. Taboada, R. Doallo, and D. Posada. 2012. jModelTest 2: more models, new heuristics and parallel computing. Nature Methods 9 (8): 772.

Decher, J., et al. 2015. Bat diversity in the Simandou Mountain Range of Guinea, with the description of a new white-winged vespertilionid. Acta Chiropterologica 17: 255–282.

Denys, C., and V. Aniskine. 2012. On a new species of *Dendromus* (Rodentia, Nesomyidae) from Mount Nimba (Guinea, West Africa). Mammalia 76: 295–308.

Denys, C., B. Kadjo, A.D. Missoup, A. Monadjem, and V. Aniskine. 2013. New records of bats (Chiroptera) and karyotypes from Guinean Mount Nimba (West Africa). Italian Journal of Zoology 80: 279–290.

Drummond, A.J., and A. Rambaut. 2007. BEAST: Bayesian evolutionary analysis by sampling trees. BMC Evolutionary Biology 7 (1): 214.

Fahr, J. 2013. *Hipposideros marisae* Aellen's leaf-nosed bat. *In* J. Kingdon (editor), Mammals of Africa, vol. 4. Hedgehogs, shrews and bats: 391–392. Oxford: Blackwells's Library Services.

Fahr, J., and N. M. Ebigbo. 2003. A conservation assessment of the bats of the Simandou Range, Guinea, with the first record of *Myotis welwitschii* (Gray, 1866) from West Africa. Acta Chiropterologica 5 (1): 125–142.

Fahr, J., H. Vierhaus, R. Hutterer, and D. Kock. 2002. A revision of the *Rhinolophus maclaudi* species group with the description of a new species from West Africa (Chiroptera: Rhinolophidae). Myotis 40: 95–126.

Findley, J.S. 1972. Phenetic relationships among bats of the genus *Myotis*. Systematic Biology 21: 31–52.

Francis, C.M. 2001. A photographic guide to mammals of South-East Asia. Sanibel Island, FL: Ralph Curtis Publishing, 128 pp.

Gray, J.E. 1821. On the natural arrangement of vertebrose animals. London Medical Repository 15 (1): 296–310.

Guindon, S., et al. 2010. New algorithms and methods to estimate maximum-likelihood phylogenies: Assessing the performance of PhyML 3.0. Systematic Biology 59 (3): 307–321.

Gunnell, G.F., R. Smith, and T. Smith. 2017. Thirty-three million year old *Myotis* (Chiroptera, Vespertilionidae) and the rapid global radiation of modern bats. PloS One 12 (3): e0172621.

Happold, M., and Happold, D.C. (editors). 2013. Mammals of Africa: hedgehogs, shrews and bats. Oxford: Blackwells's Library Services.

Hill, J.E., and P. Morris. 1971. Bats from Ethiopia collected by the Great Abbai Expedition 1968. Bulletin of the British Museum, Natural History (Zoology) 21: 27–49.

Hill, J.E., D.L. Harrison, and T.S. Jones. 1988. New records of bats (Microchiroptera) from Nigeria. Mammalia 52 (4): 590–592.

Hutterer, R., J. Decher, A. Monadjem, and J.J. Astrid. 2019. A new genus and species of vesper bat from West Africa, with notes on *Hypsugo*, *Neoromicia*, and *Pipistrellus* (Chiroptera: Vespertilionidae). Acta Chiropterologica 21: 1–22.

Ibáñez, C., J.L. García-Mudarra, M. Ruedi, B. Stadelmann, and J. Juste. 2006. The Iberian contribution to cryptic diversity in European bats. Acta Chiropterologica, 8:277–297.

International Commission on Zoological Nomenclature. 1958. Official list of generic names in zoology. London: International Trust for Zoological Nomenclature, London, 200 pp.

IUCN. 2012. IUCN Red List categories and criteria: Version 3.1, 2nd ed. Gland, Switzerland: IUCN.

Jentink, F.A. 1910. *Chrysopteron Bartelsii*, novum genus et nova species, from Java. Notes from the Leyden Museum 32:73–77.

Jiang, T., K. Sun, C. Chou, Z. Zhang, and J. Feng. 2010. First record of *Myotis flavus* (Chiroptera: Vespertilionidae) from mainland China and a reassessment of its taxonomic status. Zootaxa 2414: 41–51.

Kaup, J.J. 1829. Skizzirte Entwickelungs-Geschichte und natürliches System der europäischen Thierwelt: erster Theil welcher die Vogelsäugethiere und Vögel nebst Andeutung der Entstehung der letzteren aus Amphibien enthält. Darmstadt: In commission bei C.W. Leske.

Kawai, K., et al. 2003. The status of the Japanese and East Asian bats of the genus *Myotis* (Vespertilionidae) based on mitochondrial sequences. Molecular Phylogenetics and Evolution 28 (2): 297–307.

Kim, Y.M., et al. 2011. Complete mitochondrial genome of the Hodgson's bat *Myotis formosus* (Mammalia, Chiroptera, Vespertilionidae). Mitochondrial DNA 22 (4): 71–73.

Koopman, K.F. 1989. Systematic notes on Liberian bats. American Museum Novitates 2946: 1–11.

Koopman, K.F. 1994. Chiroptera: systematics. Handbuch der Zoologie, vol. 8 (Mammalia), pt. 60: 217 pp.

Koubínová, D., N. Irwin, P. Hulva, P. Koubek, and J. Zima. 2013. Hidden diversity in Senegalese bats and associated findings in the systematics of the family Vespertilionidae. Frontiers in Zoology 10: 48 [16 pp.]

Kunz, T.H., and S. Parsons. 2009. Ecological and behavioral methods for the study of bats, 2nd ed. Baltimore: Johns Hopkins University Press, 901 pp.

Lamotte, M., and R. Roy (editors). 2003. Le peuplement animal du Mont Nimba (Guinée, Côte d'Ivoire, Liberia). Mémoires du Muséum National d'Histoire Naturelle 190: 1–724.

Marshall, C.A.M., and W.D. Hawthorne. 2013. Important plants of northern Nimba County, Liberia. a guide to most useful, rare or ecologically important species, with Mano names and uses. Oxford Forestry Institute, Oxford, 460 pp.

McDonald, J.T., I.L. Rautenbach, and J.A.J. Nel. 1990. Roosting requirements and behaviour of five bat species at De Hoop Guano Cave, southern Cape Province of South Africa. South African Journal of Wildlife Research 20 (4): 157–161.

Mickleburgh, S., A.M., Hutson, W. Bergmans, and J. Fahr. 2008. *Hipposideros lamottei*. The IUCN Red List of Threatened Species 2008: e.T10141A3173193.

Monadjem, A., and D. K. Jacobs. 2017a. *Myotis bocagii*. The IUCN Red List of Threatened Species 2017: e.T14148A22059585.

Monadjem, A., and D. K. Jacobs. 2017b. *Myotis tricolor*. The IUCN Red List of Threatened Species 2017: e.T14207A22063832.

Monadjem, A., P.J. Taylor, W. Cotterill, and M.C. Schoeman. 2010. Bats of Southern and Central Africa. Johannesburg: Wits University Press. 596 pp.

Monadjem A, L. Richards, P.J. Taylor, and S. Stoffberg. 2013. High diversity of pipistrelloid bats (Vespertilionidae: *Hypsugo*, *Neoromicia*, and *Pipistrellus*) in a West African rainforest with the description of a new species. Zoological Journal of the Linnean Society 167 (1): 191–207.

Monadjem, A., L. Richards, and C. Denys. 2016. An African bat hotspot: the exceptional importance of Mount Nimba for bat diversity. Acta Chiropterologica 18 (2): 359–375.

Monadjem, A., P.J. Taylor, D.S. Jacobs, and F.P.D. Cotterill. 2017b. *Myotis welwitschii*. The IUCN Red List of Threatened Species 2017: e.T14211A22068792.

Monadjem, A., J.T. Shapiro, F. Mtsetfwa, A.E. Reside, and R.A. Mccleery. 2017a. Acoustic call library and detection distances for bats of Swaziland. Acta Chiropterologica 19 (1): 175–187.

Monadjem, A., et al. 2019. Systematics of West African *Miniopterus* with the description of a new species. Acta Chiropteralogica 21 (2): 237–256.

Morales, A.E., M. Ruedi, K. Field, and B. Carstens. 2019. Diversification rates have no effect on the convergent evolution of foraging strategies in the most speciose genus of bats, *Myotis*. Evolution 73 (11): 2263–2280.

Moratelli, R. 2019. Welwitsch's Myotis – *Myotis welwitschii*. *In* D.E. Wilson and R.A. Mittermeier (editors), Handbook of the Mammals of the World, vol. 9. Bats: 951. Barcelona: Lynx Edicions.

Nei, M., and S. Kumar. 2000. Molecular evolution and phylogenetics. Oxford: Oxford University Press.

Patterson, B.D., et al. 2019. Genetic variation and relationships among Afrotropical species of Myotis (Chiroptera: Vespertilionidae). Journal of Mammalogy 100 (4): 1130–1143.

Pritchard, P.C.H. 1994. Comment on the gender and declension of generic names. Journal of Mammalogy 75: 549–550.

Rambaut, A., A.J. Drummond, D. Xie, G. Baele, and M.A. Suchard. 2018. Posterior summarization in Bayesian phylogenetics using Tracer 1.7. Systematic Biology 67 (5): 901–904.

Ratcliffe, J.M. 2002. *Myotis welwitschii*. Mammalian Species 701: 1–3.

Ratcliffe, J.M., and Dawson, J.W. 2003. Behavioural flexibility: the little brown bat, *Myotis lucifugus*, and the northern long-eared bat, *M. septentrionalis*, both glean and hawk prey. Animal Behavior 66: 1–10.

Rautenbach, I.L. 1982. Mammals of the Transvaal. Ecoplan Monograph 1. Pretoria: Ecoplan Publishing.

Reid, F. 2009. A field guide to the mammals of Central America and southeast Mexico, 2nd ed. Oxford: Oxford University Press, 346 pp.

Ruedi, M., Biswas, J., and G. Csorba. 2012. Bats from the wet: two new species of Tube-nosed bats (Chiroptera: Vespertilionidae) from Meghalaya, India. Revue Suisse de Zoologie 119: 111–135.

Ruedi, M., and F. Mayer. 2001. Molecular systematics of bats of the genus *Myotis* (Vespertilionidae) suggests deterministic ecomorphological convergences. Molecular Phylogenetics and Evolution 21: 436–448.

Ruedi, M., et al. 2013. Molecular phylogenetic reconstructions identify East Asia as the cradle for the evolution of the cosmopolitan genus *Myotis* (Mammalia, Chiroptera). Molecular Phylogenetics and Evolution 69: 437–449.

Ruedi, M., G. Csorba, L.K. Lin, and C.H. Chou. 2015. Molecular phylogeny and morphological revision of *Myotis* bats (Chiroptera: Vespertilionidae) from Taiwan and adjacent China. Zootaxa 3920 (1): 301–342.

Sandberger, L., et al. 2010. Rediscovery of the Liberian Nimba toad, *Nimbaphrynoides liberiensis* (Xavier, 1978) (Amphibia: Anura: Bufonidae), and reassessment of its taxonomic status. Zootaxa 2355: 56–68.

Schoeman, M.C., and D.S. Jacobs. 2008. The relative influence of competition and prey defenses on the phenotypic structure of insectivorous bat ensembles in southern Africa. PLoS One 3 (11): e3715.

Schoeman, M.C., and K.J. Waddington. 2011. Do deterministic processes influence the phenotypic patterns of animalivorous bat ensembles at urban rivers? African Zoology 46 (2): 288–301.

Shapiro, J., and R. Cooper-Bohannon. 2020. *Rhinolophus guineensis*. The IUCN Red List of Threatened Species 2020: e.T19542A21980043.

Simmons, N.B. 2005. Order Chiroptera. *In* D.E. Wilson and D.M Reeder (editors), Mammal species of the world: a taxonomic and geographic reference, 3rd ed., vol. 1: 312–529. Baltimore: Johns Hopkins University Press.

Simmons, N.B., and A.L. Cirranello. 2020. Bat species of the world: a taxonomic and geographic database. Online resource (https://batnames.org), accessed February 4, 2020.

Skinner, J.D., and R.H.N. Smithers. 1990. The mammals of the southern African subregion, 2nd ed. Pretoria: University of Pretoria.

Smith, M.F., and J.L. Patton. 1993. Diversification of South American muroid rodents: evidence from mitochondrial DNA sequence data for the Akodontine tribe. Biological Journal of the Linnean Society 50: 149–177.

Smithers, R.H.N. 1983. The mammals of the southern African subregion. Pretoria: University of Pretoria, 736 pp.

Smithers, R.H.N., and V.J. Wilson. 1979. Check list and atlas of the mammals of Zimbabwe Rhodesia. Museum Memoires of the National Museums and Monuments of Rhodesia 9: 1–193.

Stadelmann, B., et al. 2004b. Molecular Systematics of the Fishing Bat Myotis (*Pizonyx*) *vivesi*. Journal of Mammalogy 85: 133–139.

Stadelmann, B., D.S. Jacobs, C. Schoeman, and M. Ruedi. 2004a. Phylogeny of African *Myotis* bats (Chiroptera, Vespertilionidae) inferred from cytochrome b sequences. Acta Chiropterologica 6: 177–192.

Stadelmann, B., Kunz, T.H., Lin, L.K., and M. Ruedi. 2007. Molecular phylogeny of New World *Myotis* (Chiroptera, Vespertilionidae) inferred from mitochondrial and nuclear DNA genes. Molecular Phylogenetics and Evolution 43: 32–48.

Stamatakis, A. 2014. RAxML version 8: a tool for phylogenetic analysis and post-analysis of large phylogenies. Bioinformatics 30 (9): 1312–1313.

Stoffberg, S., and D.S. Jacobs. 2004. The influence of wing morphology and echolocation on the gleaning ability of the insectivorous bat *Myotis tricolor*. Canadian Journal of Zoology 82 (12): 1854–1863.

Tamura, K., and M. Nei. 1993. Estimation of the number of nucleotide substitutions in the control region of mitochondrial DNA in humans and chimpanzees. Molecular Biology and Evolution 10 (3): 512–526.

Tate, G.H.H. 1942. Results of the Archbold Expeditions, no. 47: review of the vespertilionine bats, with special attention to genera and species of the Archbold collections. Bulletin of the American Museum of Natural History 80 (7): 221–297.

Taylor, P.J. 1991. First record of Welwitsch's hairy bat (*Myotis welwitschii*) from Natal. Durban Museum Novitates 16: 35–36.

Taylor, P.J. 1998. The smaller mammals of Kwazulu-Natal. Pietermaritzburg: University of Natal Press, 139 pp.

Taylor, P.J. 2000. Bats of southern Africa – guide to biology, identification, and conservation. Pietermaritzburg: University of Natal Press. 206 pp.

Tsytsulina, K., M.H. Dick, K. Maeda, and R. Masuda. 2012. Systematics and phylogeography of the steppe whiskered bat *Myotis aurascens* Kuzyakin, 1935 (Chiroptera, Vespertilionidae). Russian Journal of Theriology 11: 1–20.

Weyeneth, N., S.M. Goodman, S. and M. Ruedi. 2011. Do diversification models of Madagascar's biota explain the population structure of the endemic bat *Myotis goudoti* (Chiroptera: Vespertilionidae)? Journal of Biogeography, 38: 44–54.

Wieringa, J.J., and L. Poorter. 2004. Biodiversity hotspots in West Africa, patterns and causes. 61–72 *In* L. Poorter, F. Bongers, F.N. Kouame, and W.D. Hawthorne (editors), Biodiversity of West African forests. An ecological atlas of woody plant species. Oxford: Cabi Publishing, 528 pp.

Woodman, N. 1993. The correct gender of mammalian generic names ending in *-otis*. Journal of Mammalogy 74 (3): 544–546.

APPENDIX 1

Specimens Examined

The following list includes all specimens used in the morphological components of this study with data on their respective localities. See Materials and Methods for institutional abbreviations.

Myotis morrisi (*N* = 1). ETHIOPIA— Blue Nile Gorge, Mouth of Didessa River, Forward Base Three (BMNH 70.488 [holotype]).

Myotis nimbaensis (*N* = 2). GUINEA—Nimba Mountains, Kaiser Adit 2, N07.66499, W008.37223 (AMNH 279589 [holotype], 279590 [paratype]).

Myotis tricolor (*N* = 28). ETHIOPIA— Amhara Region, Agew Awi Zone, Dangila (BMNH 37.2.24.13); KENYA—Rift Valley Province, 20 mi. SW of Kitale, R. Barberton Farm (USNM 351060, 351061); Rift Valley Province, Crater of Mt. Menengai, 7400 ft. (USNM 317927, 317928); Rift Valley Province, 3mi NW Nakuru, Menengai Crater, 6500 ft. (BMNH 75.2549—75.2554); Rift Valley Province, West Pokot County, Sigor, Wei-Wei River (BMNH 75.2555); LIBERIA—Grand Cape Mt., Bomi wood concession (AMNH 257053); MALAWI—Zomba District, Zomba (BMNH 87.1082); SOUTH AFRICA—Eastern Cape Province, King William's

Town (AMNH 146789); KwaZulu-Natal, Estcourt, Will Brook (BMNH 14.5.4.2); KwaZulu-Natal, Otto's Bluff (AMNH 232029, 232030); KwaNatal, Pietermaritzburg, Town Bush (USNM 292066); Mpumalanga Provence, Barberton, Louws Creek [= Low's Creek] (USNM 238099); Transvaal, 32 mi W of Pretoria, Uitkomst Farm (USNM 342643—342645); Transvaal, Kruger National Park, ca. 4 km east of Skukuza (AMNH 257358); UGANDA—Sebai District, Near Sipi, Cave at Kyema (BMNH 64.172); Mt. Elgon, Kapretwa (BMNH 40.740, 40.741); ZAMBIA—Cave near Mujimbe Hill (AMNH 89776).

Myotis welwitschii (*N* = 3). MALAWI—Southern Region, Cholo [= Thyolo], Ruo River (BMNH 22.12.17.75); Southern Region, Near Chiromo (BMNH 22.12.17.76); SOUTH AFRICA—Transvaal, 50 miles ENE of Lydenburg (BMNH 0.11.6.1).

APPENDIX 2

Sources of Molecular data

Species included in phylogenetic analyses, sampling localities, and GenBank accession for cytochrome *b* sequences employed in this study.

Species	Locality	GenBank	Reference
M. nimbaensis	Guinea	MT427587	This study
M. nimbaensis	Guinea	MT427588	This study
M. albescens	Bolivia	AF376839	Ruedi and Mayer, 2001
M. anjouanensis	Comoros	GU116765	Weyeneth et al., 2011
M. bechsteinii	Switzerland	AF376843	Ruedi and Mayer ,2001
M. blythii	Kirghizstan	AF376840	Ruedi and Mayer, 2001
M. bocagii bocagii	Ghana	AJ504408	Stadelmann et al., 2004a
M. bocagii cupreolus	Tanzania	KF312502	Ruedi et al., 2013
M. brandtii	Russia	AM261886	Stadelmann et al., 2007
M. chinensis	China	EF555227	Jiang et al., 2010
M. chinensis	China	EF555228	Jiang et al., 2010
M. emarginatus	Greece	AF376849	Ruedi and Mayer, 2001
M. fimbriatus	China	KF312517	Ruedi et al., 2013
M. formosus sensu stricto	Taiwan	KF312518	Ruedi et al., 2013
M. formosus sensu stricto	China	EF555233	Jiang et al., 2010
M. formosus sensu stricto	Taiwan	EU434932	Jiang et al., 2010
M. rufoniger	Taiwan	EU434933	Jiang et al., 2010

APPENDIX 2 *continued*

Species	Locality	GenBank	Reference
M. rufoniger	Taiwan	KF312519	Ruedi et al., 2013
M. rufoniger	China	EF555234	Jiang et al., 2010
M. rufoniger	China	EF555235	Jiang et al., 2010
M. rufoniger	Korea	AB106592	Kawai et al., 2003
M. rufoniger	Laos	AJ841950	Stadelmann et al., 2004a
M. rufoniger	Korea	HQ184048	Kim et al., 2011
M. frater	Japan	AB106593	Kawai et al., 2003
M. goudoti	Madagascar	AJ504451	Stadelmann et al., 2004a
M. goudoti	Madagascar	GU116756	Weyeneth et al.,2011
M. goudoti	Madagascar	GU116761	Weyeneth et al., 2011
M. goudoti	Madagascar	GU116762	Weyeneth et al., 2011
M. goudoti	Madagascar	GU116768	Weyeneth et al., 2011
M. latirostris	Taiwan	AM262330	Stadelmann et al., 2007
M. pilosus	China	AJ504452	Stadelmann et al., 2004b
M. ruber	Brazil	AF376867	Ruedi and Mayer, 2001
M. scotti	Ethiopia	AJ841958	Stadelmann et al., 2004a
M. tricolor	South Africa	AJ841952	Stadelmann et al., 2004a
M. tricolor	South Africa	AJ841953	Stadelmann et al., 2004a
M. welwitschii	South Africa	AF376874	Ruedi and Mayer, 2001
M. welwitschii	Guinea	AJ841954	Stadelmann et al., 2004a
M. welwitschii	Uganda	AF376873	Ruedi and Mayer, 2001
Kerivoula papillosa	Malaysia	EU188782	Anwarali Khan et al., 2010
Murina cyclotis	Laos	JQ044692	Ruedi et al., 2012
Murina cyclotis	India	JQ044689	Ruedi et al., 2012
M. albescens	Peru	MK799657	Patterson et al., 2019
M. aurascens	South Korea	AY665145	Tsytsulina et al., 2012
M. blythii	Pakistan	MK799658	Patterson et al., 2019
M. blythii	Greece	KF312501	Ruedi et al., 2013
M. bocagii	Tanzania	MK799666	Patterson et al., 2019
M. bocagii	Dem. Rep. Congo	MK799659	Patterson et al., 2019
M. bocagii	Dem. Rep. Congo	MK799660	Patterson et al., 2019
M. bocagii	Kenya	MK799661	Patterson et al., 2019
M. bocagii	Kenya	MK799662	Patterson et al., 2019
M. bocagii	Kenya	MK799663	Patterson et al., 2019

APPENDIX 2 *continued*

Species	**Locality**	**GenBank**	**Reference**
M. bocagii	Kenya	MK799664	Patterson et al., 2019)
M. bocagii	Kenya	MK799665	Patterson et al., 2019
M. bocagii	Unknown	MF038469	Patterson et al., 2019
M. bocagii	Senegal	JX276105	Koubinová et al., 2013
M. emarginatus	Jordan	MK799667	Patterson et al., 2019
M. formosus	Taiwan	KP187859	Ruedi et al., 2015
M. formosus	Taiwan	KP187860	Ruedi et al., 2015
M. frater	Madagascar	KP187872	Ruedi et al., 2015
M. goudoti	Madagascar	MK799668	Patterson et al., 2019
M. goudoti	Madagascar	MK799669	Patterson et al., 2019
M. goudoti	Madagascar	MK799670	Patterson et al., 2019
M. goudoti	Madagascar	MK799671	Patterson et al., 2019
M. goudoti	Madagascar	MK799672	Patterson et al., 2019
M. goudoti	Madagascar	GU116767	Weyeneth et al., 2011
M. laniger	Taiwan	KP187877	Ruedi et al., 2015
M. mystacinus	Germany/Switzerland	AF376861	Ruedi and Mayer, 2001
M. rufoniger	Taiwan	KP187882	Ruedi et al., 2015
M. rufoniger	Taiwan	KP187881	Ruedi et al., 2015
M. secundus	Taiwan	KP187887	Ruedi et al., 2015
M. tricolor	South Africa	MK799682	Patterson et al., 2019
M. tricolor	South Africa	MK799683	Patterson et al., 2019
M. tricolor	South Africa	MK799684	Patterson et al., 2019
M. tricolor	South Africa	MK799685	Patterson et al., 2019
M. tricolor	Kenya	MK799674	Patterson et al., 2019
M. tricolor	Kenya	MK799675	Patterson et al., 2019
M. tricolor	Kenya	MK799702	Patterson et al., 2019
M. tricolor	Kenya	MK799676	Patterson et al., 2019
M. tricolor	Kenya	MK799703	Patterson et al., 2019
M. tricolor	Kenya	MK799677	Patterson et al., 2019
M. tricolor	Kenya	MK799704	Patterson et al., 2019
M. tricolor	Kenya	MK799678	Patterson et al., 2019
M. tricolor	Kenya	MK799705	Patterson et al., 2019
M. tricolor	Kenya	MK799706	Patterson et al., 2019
M. tricolor	Kenya	MK799679	Patterson et al., 2019

APPENDIX 2 *continued*

Species	**Locality**	**GenBank**	**Reference**
M. tricolor	Kenya	MK799680	Patterson et al., 2019
M. tricolor	Uganda	MK799686	Patterson et al., 2019
M. tricolor	Uganda	MK799687	Patterson et al., 2019
M. tricolor	Uganda	MK799688	Patterson et al., 2019
M. tricolor	Uganda	MK799689	Patterson et al., 2019
M. tricolor	Uganda	MK799690	Patterson et al., 2019
M. tricolor	Kenya	MK799681	Patterson et al., 2019
M. tricolor	South Africa	AJ504409	Stadelmann et al., 2004a
M. welwitschii	Malawi	MK799697	Patterson et al., 2019
M. welwitschii	Malawi	MK799698	Patterson et al., 2019
M. welwitschii	Kenya	MK799692	Patterson et al., 2019
M. welwitschii	Kenya	MK799693	Patterson et al., 2019
M. welwitschii	Kenya	MK799694	Patterson et al., 2019
M. welwitschii	Kenya	MK799695	Patterson et al., 2019
M. welwitschii	Kenya	MK799696	Patterson et al., 2019
M. welwitschii	Tanzania	MK799699	Patterson et al., 2019
M. welwitschii	Tanzania	MK799700	Patterson et al., 2019
M. welwitschii	Tanzania	MK799701	Patterson et al., 2019
M. welwitschii	Kenya	MK799691	Patterson et al., 2019
Kerivoula lanosa	Kenya	MK799656	Patterson et al., 2019
Miniopterus aelleni	Madagascar	MK799655	Patterson et al., 2019

All issues of *Novitates* and *Bulletin* are available on the web (http://digitallibrary.amnh.org/dspace). Order printed copies on the web from:
http://shop.amnh.org/a701/shop-by-category/books/scientific-publications.html

or via standard mail from:
American Museum of Natural History—Scientific Publications
Central Park West at 79th Street
New York, NY 10024

∞ This paper meets the requirements of ANSI/NISO Z39.48-1992 (permanence of paper).